Feasibility Study on Perovskite Solar Cell for Space Application through Ground and In-Orbit Tests

KYUSHU INSTITUTE OF TECHNOLOGY

Doctorate Degree in Space Systems Engineering

Izrael Zenar Bautista

Feasibility Study on Perovskite Solar Cell for Space Application through Ground and In-Orbit Tests

Thesis Adviser:

Mengu Cho, PhD

Panel:

Tingli Ma, PhD

Mitsuru Imaizumi, PhD

Kazuhiro Toyoda, PhD

Kentaro Kitamura, PhD

Date of Submission

December 2021

Feasibility Study on Perovskite Solar Cell for Space Application through Ground and In-Orbit Tests

Thesis by

Izrael Zenar Bautista

Submitted to the Graduate School of Engineering
Department of Applied Science for Integrated System Engineering
Kyushu Institute of Technology

In Partial Fulfilment of the Requirements
For the Doctoral of Philosophy in
Space System Engineering

December 2021

Acknowledgement

First and foremost, I would like to express my heartfelt thanks to the Lord God for the strength, wisdom and blessings he has given me during the time I am doing this thesis. Next I would like to thank my parents, Ariel Bautista and Zenaida Bautista for supporting me in this endeavor and to Mia Perez who's always there to cheer me up and help me in the revisions and proof-reading of this thesis.

I'd also like to thank my supervisor, Prof. Mengu Cho, and our collaborator from Graduate Life Science of Kyutech, Wakamatsu campus, Dr. Tingli Ma and her student Shuzhang Yang from which the perovskite solar cell samples came from. The members of the panel, Dr. Kentaro Kitamura, Dr. Mitsuru Imaizumi and Dr. Kazuhiro Toyoda for the guidance and comments that lead to finishing this thesis. The senseis, students and staff of LaSEINE laboratory for their invaluable guidance and help during my stay in Kyutech.

To the BIRDS-4 team whom I formed very close bonds with during the time we are making the satellites. The camaraderie, friendship and times we have shared has kept me going through the difficult times during my study in Japan. Finally, I'd like to thank the Department of Science and Technology – Science Education Institute for the support and funding through the STAMINA4SPACE program – STeP-UP project.

To God be the glory!

Abstract of Thesis

Solar energy is used by majority of spacecraft and satellites as their source of power using triple-junction solar cells which have high power conversion efficiency but expensive making the idea of space infrastructures like space solar power plant and space factories economically unviable. The emergence of organic-inorganic metal halide Perovskite solar cells (PSCs) in 2009 lead to the development of lightweight and cost-efficient solar energy converter that has achieved record efficiency of 25.6% for single junction and 29.5% for tandem cells, as of the writing of this paper. Due to its high conversion efficiency and high power density, it is seen as a viable candidate to be used in satellites and spacecraft. This paper discusses the ground tests and the on-orbit demonstration of Perovskite solar cell with different hole-transport material that would verify the feasibility of Perovskite solar cell in space. Ground test results showed HTM free PSCs made with Carbon as back electrode have better stability than PSC with organic and inorganic HTM, albeit HTM free PSC has lower power conversion efficiency. In-orbit data was only obtained for the inorganic CuSCN HTM which showed slower degradation in space compared with the ground test done on fresh samples. Ageing of the PSCs prior to launch to space is pointed as the cause of slower degradation that allowed for stabilization of materials and reduced reaction with the environment and was demonstrated when ground tests were repeated on aged cells. Comparison between the ground test and in-orbit data showed different degradation rate values, hence improvements to ground test methodology and in-orbit data gathering were discussed to possibly arrive at the same value. Based on the derived lifetime of Perovskite solar cells in ground test and in-orbit, the tested CuSCN samples are not yet ready for space applications. Improvements in materials used, as well as encapsulation method is needed to be developed to allow PSC's future use in space.

Keywords: Perovskite, solar, satellite energy

Contents

List of Figures

List of Tables

Chapter 1: Introduction

1.1 Background of the study

Current satellites and spacecrafts use triple-junction solar cells as power source because of its stability, ease of integration with other systems, and high power conversion efficiency. The typical efficiency for this type of solar cell is 32% and the highest recorded is 37.9% [1]. This is significantly higher than the commercial terrestrial silicon solar cells being used in solar farms with efficiencies ranging from 14 to 25% with the highest recorded efficiency at 26.1% [2]. For projects such as space based solar power and space factories, high efficiency solar cells with high power density are preferred to harness more energy per area per unit mass. The downside to this type of solar cell is the cost as it costs around 300 USD per watt, which is more than 130 times larger than the commercial terrestrial solar cells making it economically infeasible to make these infrastructures. [3]

Thus, this presents the need to explore alternative solar cell technologies that cost less than a triple-junction solar cell but with the same or higher power conversion efficiency and power density. Cheaper solar cells will bring down the cost in assembling satellites and other future space infrastructures while improving efficiency and power denser solar cells will reduce overall satellite or space infrastructure mass. Reducing the mass also translates to savings for launch cost and would make large space infrastructure projects mentioned earlier realizable.

In 2009, organic-inorganic metal halide perovskite as a solar cell material started started a new avenue for research in the field of renewable energy [4]. As of writing of this paper, record efficiencies of 25.6% for single junction type and 29.5% for tandem cells have been reached in laboratory setting [5], and a theoretical maximum conversion efficiency of 45.3%

in a tandem architecture [6]. Perovskite solar cells have a distinct advantage over multi-junction solar cells due to their higher power density [7], cheaper production cost [8] and higher tolerance to radiation [9]. Unfortunately, disadvantages such as instability, hysteresis and toxicity continue to challenge the commercialization of PSCs. Exposure to oxygen and moisture is a major factor for instability and short lifespan, which are absent in space [10] [11]. The potential of PSCs in space and the challenges for its implementation were discussed in a recent article by Yang et al. [12]. The performance of PSC under different environmental conditions which results to the degradation of its parameters have also been discussed by various articles [9] [13] [14]. Shown in Table 1 is a comparison of different parameters of commercial triple junction solar cell and Perovskite solar cell.

Table 1 Comparison of triple junction solar cell and perovskite solar cell

	Triple junction solar cell	Perovskite solar cell
Efficiency	37.9%	25.6%(single junction); 29.5%(tandem)
Cost per Watt	~$300	~$0.127
Specific power (kW/kg)	~3.6	~23
Stability	Very stable	Unstable under atmospheric environment
Safety	Generally safe	Contains Pb

Hole transport material (HTM) acts as the physical and energy barrier between the perovskite layer and the electron transport layer. They increase the efficiency of PSCs by providing higher hole mobility towards the electrode which collects the holes. Hole transport layers also help in preventing the degradation of the perovskite layer as it covers and protects it also from the environment [15]. Hole transport materials can be categorized into three main groups: Organic, Inorganic and Carbonaceous material. In this research, we used Spiro-

OMeTAD as organic HTM, CuSCN as inorganic HTM and instead of using Carbonaceous material, a hole transporter free Carbon back electrode is used. Table 2 outlines the difference between the HTMs studied in this research in terms of their price per gram and energy level. The matched energy level of the three HTMs with the Perovskite material enables their usage in this study.

Table 2 Comparison of HTMs used in the research

	Price/gram ($) [16]	Energy level (eV)
Spiro-OMeTAD (Organic)	347.000	-5.3 ~ -2.3
CuSCN (Inorganic)	1.652	-5.3 ~ -1.5
Carbon (HTM free)	0.915	-5.0

In-orbit demonstration of new technologies is an important step towards the use of these new technologies for future space missions. In this research, this step is taken by attaching PSCs to a constellation of CubeSats that are part of the 4th Joint Global Multi-Nation Birds Project or BIRDS-4.

The thesis is organized as follows: In Chapter 2, published articles were reviewed discussing perovskite solar cells and their hole transport material that are focused in the study. Related works on various environment tests and space experiments are also discussed. Fabrication and characterization of the PSCs are discussed in Chapter 3, while Chapter 4 discusses the space environment test methodologies and how PSCs made of different types of HTM, or lack thereof, perform under these simulated space environments. The results of the BIRDS-4 Perovskite solar cell mission are presented in Chapter 5. Comparison of the ground test results and in-orbit data is done in Chapter 6 and finally concluding remarks and recommendations for future work are presented in Chapter 7.

1.2 Research Purpose

The purpose of this research is to identify the feasibility of current Perovskite solar cell technology for space applications and identify the best hole transport material to use in space by gathering data on their performance under simulated space environment and actual space environment

Most published literature only discuss single type of cell exposed in single environment which is usually earth environment. On the other hand, this research tests multiple types of PSC and exposed in multiple space environment conditions. This allows understanding which material would be best towards the goal of space utilization of PSCs.

The research focuses on the current state-of-art of perovskite and not in engineering/designing a new perovskite solar cell

1.3 Objectives

As part of the research towards the use of Perovskite solar cells as energy source for space applications, this paper investigates the capability of Perovskite solar cells and hole transport materials of interest's performance under space environment. It is done thru simulated space environment tests that mimics the conditions that a satellite deployed in low-earth orbit from the International Space Station would experience. The results of these tests would then be compared with in-orbit data gathered through the BIRDS-4 Perovskite solar cell demonstration satellite mission.

The following objectives outline the milestones towards the purpose of this study:

1. To obtain data to predict the performance of current PSC technology in LEO space environment in simulated space environment (ground test)
2. To obtain and analyze in-orbit data on performance of PSC thru BIRDS-4 satellites' PSC mission
3. To compare in-orbit data with ground data to identify feasibility of PSC for space applications and verify if ground test methodology simulates actual PSC performance and degradation in space

By comparing the performance of PSCs with different hole transport material (HTM) under space qualification tests and in-orbit data, we can identify which material is best used for space applications. The ground test results would also allow verification on the difference or similarity of ground test methodology against actual data taken in space environment. This research would also give insight on the performance of Perovskite solar cells in space and serve as reference for future research in this field.

1.4 Novelty

The case for novelty of the study is that existing research on the ability of perovskites in space applications has only done using stratospheric balloon flight and suborbital rocket flight which are both short term experiments.

This study is the first demonstration of PSC in a nanosatellite which will provide long term data and enable analysis on the performance PSCs in actual space environment on board a cubesatellite. From the reviewed literature, a stratospheric balloon flight which lasted for 3 hours and a suborbital rocket flight which lasted for 6 minutes are the only data gathering done

that are space related. This study covers 5 months' worth of in-orbit data allowing for better understanding of the effects of space environment on PSC.

Chapter 2: Related Work

2.1 Perovskite solar cell

Perovskite is a general term for compounds having a crystal structure similar $CaTiO_3$ ABX_3, where A – is a big cation, B – a smaller cation and X – an anion which bonds to both cations [17]. It is named after the Russian mineralogist Lev Perovski by its's discoverer, German mineralogist Gustav Rose [18]. In 2009, Miyasaka et al. made a synthetic Perovskite material as light absorber material in TiO_2 similar to dye sensitized solar cell architecture which achieve a power conversion efficiency (PCE) of 3.8% but was highly unstable and quickly deteriorated [4]. Then in 2012, Mike Lee and Henry Snaith used solid-state hole transporter such as Spiro-OMeTAD and achieved conversion efficiencies of more than 10% [19]. Research has since exponentially grown as shown in Figure 1. The estimated cost of mass production of Perovskite solar cells could be as low as $\$37/m^2$ according to [8]. One of the drivers for the low cost of production is the capability of manufacturing PSCs in flexible substrates which enables high throughput roll-to-roll manufacturing process. The article mentions the three main

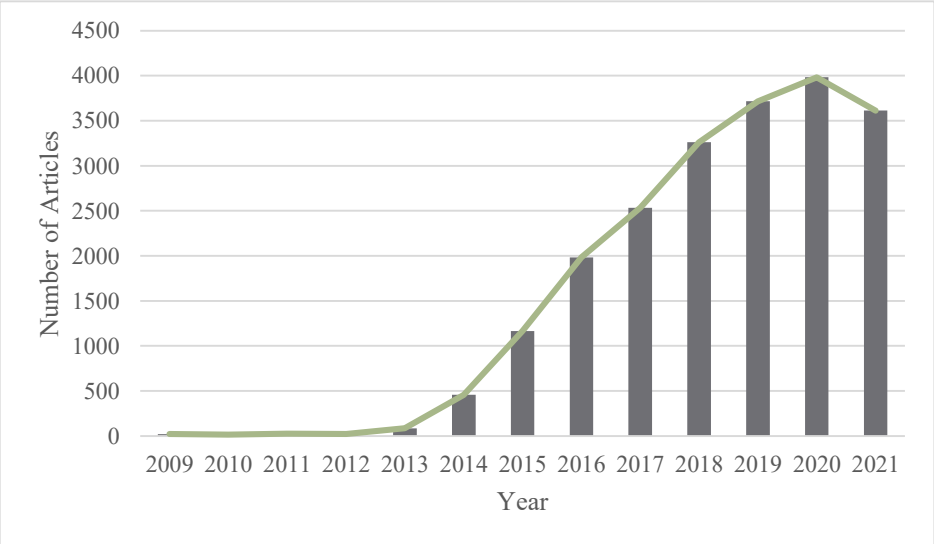

Figure 1 Publications related to Perovskite solar cell taken from Scopus, October 2021 using keywords "Perovskite solar cell".

barriers to commercialization of PSCs: high cost of HTM materials, screen printing process of the back electrode and transparent front conductor (ITO/FTO).

Perovskite solar cells produce energy in the following process illustrated in Figure 2 [20] [21]:

1. Absorption of light and generation of excitons – excited electron-hole pairs which contain energy waiting to be released.

2. Diffusion of excitons – the excitons diffuse towards the charge extraction layers

3. Dissociation of excitons and generation of charges – the excitons dissociate producing charge carriers (electrons and holes).

4. Charge transportation and collection – the electrons and holes produced are collected by the charge transportation layers: electron transporting layer (ETL) and hole transport layer (HTL). These electrons and holes migrates to the anode and cathode of the solar cell to produce current

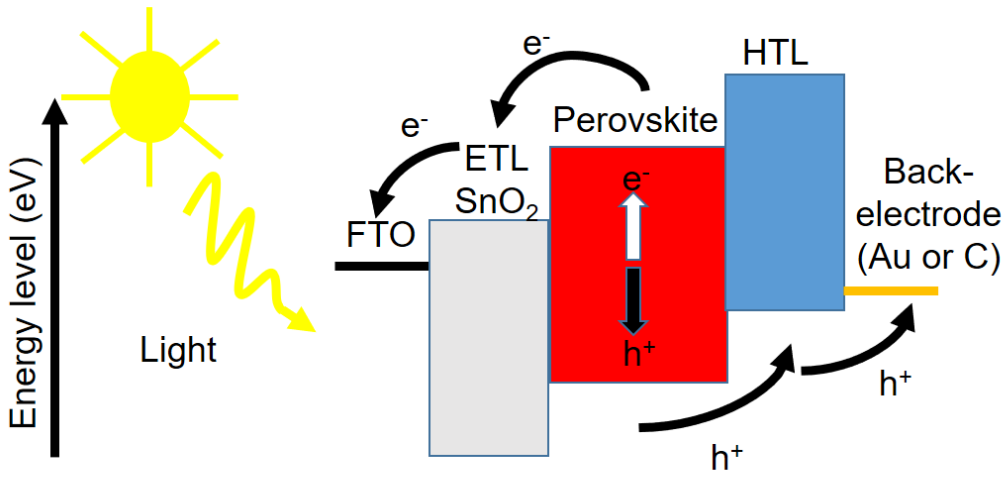

Figure 2 Energy level diagram of the main process of energy production of PSCs

2.1.1 Hole transport material

A comprehensive review article by Pitchaiya et al [15] on various HTMs used in PSCs based on several research articles outlined a detailed comparison of the HTMs based on cost and device performance (efficiency and stability). A significant number of articles use organic HTMs such as Spiro-OMeTAD (2,2',7,70-Tetrakis(N,N-di-(4-methoxyphenyl)amino)-9,9'-spirobifluorene), due to its ionization potential, solubility, solid-state morphology and absorption spectrum [22]. This allowed for fabrication of PSCs with high open-circuit voltage and high efficiencies [23].

Dye sensitized solar cells (DSSCs) first demonstrated the use of Spiro-OMeTAD as HTM in 1998 where it achieved a PCE of 2.56% in a laboratory [24]. A major disadvantage of using this material is its high cost and instability [25]. An inexpensive, abundant, non-toxic and low energy extensive material was sought to replace organic HTMs which led to the use of Cuprous thiocyanate or CuSCN as inorganic HTM by Chavhan et al. and achieved PCE of 6.4% [26]. The wider band gap, high conductivity and hydrophobic property of Inorganic HTMs allowed for a more cost efficient and stable device fabrication [27] [28]. Perovskite solar cells using inorganic HTM displayed lower power conversion efficiency than those using organic HTM. The high cost of gold as back electrode material lead to the identification of Carbon materials as replacement since it also has good conductivity with lower cost compared to gold. Carbon materials also became a potential material to remove the need for HTM since it has a work function value of ~5.0 eV [29] [30].

2.1.2 Simulated environment tests on Perovskite solar cells

Several articles have been published which tests the ability of PSCs to survive in various environment. Miyazawa et al. [9] evaluated the space radiation tolerance of PSC under electron and proton beam while also testing if PSCs and concluded that PSCs can endure the extreme temperature of space. Sheikh et al [13] and Schwenzer et al [31] looked into the effect of temperature cycling in the performance decline of PSC and found irreversible reduction to the performance of PSC due to deterioration of interfacial carrier and ion accumulation at the contacts due to temperature dependent changes in the built-in field of the PSC as the cause of decline in performance. The effect of UV light was investigated by Zhao and Park [32]and Leijtens et al [33] and found that UV light reduces the performance of PSCs due to the photocatalytic reaction of commonly used electron transport layer TiO_2 to UV light which creates trap sites and triggers recombination of carriers produced by the perovskite layer. On the otherhand, Lee et al [14] and found its restorative effect on PSC material by resolving of stacked charges and defect state neutralization. Vacuum induced degradation is discussed by Hofstetter et al [34]which is due to the formation of metallic lead species largely due to the organic cation used as HTM. Jiang et al [35] found vacuum accelerates the ion migration and transformation of material and comes up with a mitigation structure to prevent degradation due to vacuum.

2.1.3 Solar cells sent to Space

CubeSats or nanosatellites have been used to allow a cheaper way to demonstrate and gather data on actual in-orbit performance of new types of solar cells in space. The XI-V CubeSat from University of Tokyo demonstrated $Cu(In,Ga)Se_2$ (CIGS) solar cells and GaAs solar cells [36]. The Small demonstration satellite (SDS-1) by the Japanese Aerospace

Exploration Agency (JAXA) was used to demonstrate their thin film dual junction (TF2J) InGaP/GaAs solar cell and CIGS [37]. The first demonstrated dual-junction solar cells in space was done by Horyu-II from Kyushu Institute of Technology [38].

Perovskite cells have also been tested in extra-terrestrial environment. Cardinaletti et al [39] attached PSCs in a stratospheric weather balloon which recorded the performance of the cells every 20 seconds until it reached a height of 32 km for 3 hours. Encapsulation failure which lead to degradation of the active layer and the charge transport layers was determined as the cause of loss of function of the devices attached and the main conclusion from their study is that PSCs are highly affected by extreme temperature and future research should focus in improving this area. Perovskite solar cells have also been attached to a suborbital rocket reaching a height of 240km for a total measurement time of 6 minutes. An efficiency performance of 14mW/cm^2 was measured under varying light intensity [40]. This ex-situ demonstration shows that PSCs are suitable not just for near-Earth application, but deep space satellite missions as well. Manufacturing PSC outside earth was discussed in an article published by NASA thru electrospraying which is similar to inkjet printing. This technology would enable astronauts to build solar cells as they explore [41]. Hence, PSCs are not limited to low-earth orbit applications, but also in deep-space and space exploration applications.

Chapter 3: Research Methodology and Perovskite fabrication

The general flow of the methodology of the thesis is presented in Figure 3. The three (3) types of Perovskite solar cell with different hole transport material (Spiro-OMeTAD, CuSCN, and Carbon as HTM and back electrode) are fabricated by Ma laboratory from the Kyushu Institute of Technology, Wakamatsu campus' Graduate School of Life Science and Systems Engineering. They fabricated and supplied all the samples used in this research. Samples fabricated are initially tested for their initial parameters then encapsulated to protect the Perovskite material from the atmospheric environment. The samples with the highest power conversion efficiency are chosen to be attached to the satellite that will go into space while the remaining samples are used for the simulated space environment test. Data are gathered from samples that were attached to the satellites launched to space are gathered through the BIRDS-4 project's Perovskite solar cell mission. These data are analyzed and processed for the lifetime prediction and compared with the ground test results.

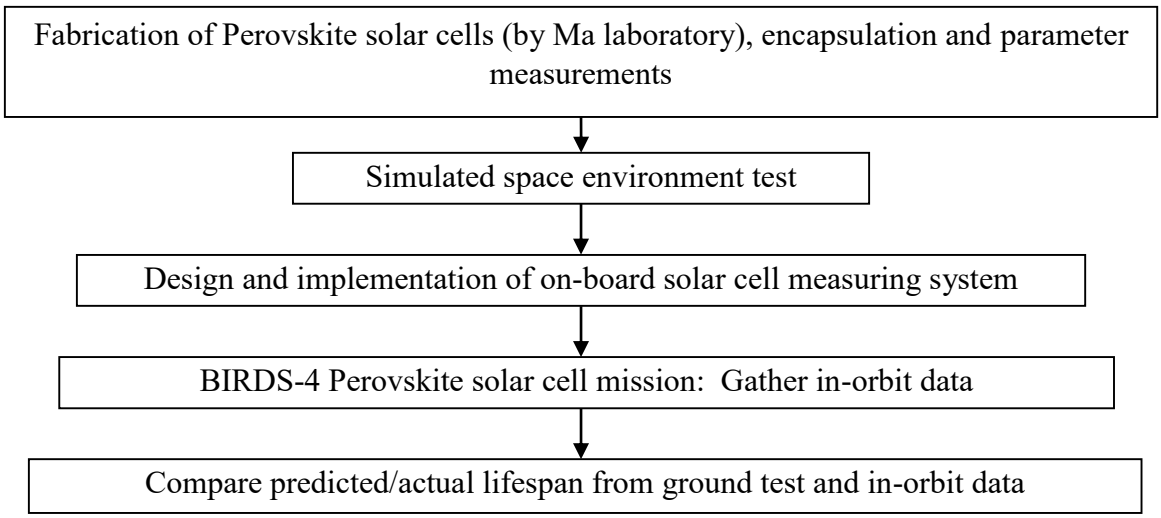

Figure 3 General flowchart of the methodology of the thesis

3.1 Perovskite solar cell fabrication and encapsulation

The Perovskite solar cells fabricated by Ma laboratory is a triple cation perovskite layer which follows an n-i-p planar architecture in the following order from the source of light: Glass/Indium Tin Oxide (ITO)/Tin Oxide (SnO_2)/ $FA_{0.81}MA_{0.10}Cs_{0.04}PbI2.55Br0.40$ /HTM (Organic, Inorganic and HTM free for carbon type)/back electrode (Gold or Carbon paste). A superstrate made with 20x20 mm soda lime glass already doped with 100±20 nm of ITO is procured. Acetone and ethanol were used to remove foreign substances from the ITO soda lime glass surface before depositing Tin oxide (SnO2) to the ITO glass. Spin coating and heating process are done inside a glove box. The triple cation perovskite is made using 800 µL of Dimethylformamide, 200 µL of Dimethyl sulfoxide, 0.0182 g of CsI, 0.2046 g of FAI, 0.0235 g of MABr, 0.0771 g $PbBr_2$ and 0.6067 g of PbI_2 mixed using a shaker to make the Perovskite solution. The organic Spiro-OMeTAD HTM is made with 72.3 mg Spiro-OMeTAD and 1mL clorobenzen while the inorganic CuSCN HTM layer is made with 35 mg CuSCN and 1mL Diethyl disulphide. For the HTM free PSC, it uses a Graphite – Carbon paste to transport the holes as well as serve as back electrode material, instead of gold. The ITO doped glass/SnO_2 is layered with 50 µL of Perovskite solution using spin coating. The superstrate is then heated using a hot plate at 150°C to evaporate the solvents evaporate and allow the formation of the dark Perovskite material crystals. After that, the HTM solution (organic and inorganic) is then spin coated on the Perovskite cell and heated using hot plate at 100°C. For the PSCs with organic and inorganic HTM, gold is deposited using vacuum deposition. In the case of the HTM free PSC, after adding the perovskite layer, the cells are taken out of the glove box and carbon paste is applied on the PSC and allowed to dry for a few minutes. Each ITO glass contains 3 individual samples. For the final samples attached to the satellites, the cells were cut

to 12x20 mm leaving two samples for each cell. Each satellite carries two samples of each type of HTM and HTM free PSC.

The following materials are procured from sigma aldrich: Dimethylformamide, Spiro-OMeTAD, Chlorobenzene, CuSCN, Diethyl disulfide, Dimethyl sulfoxide, CsI, MABr, $PbBr_2$, PbI_2.

The fabricated PSCs are then encapsulated to increase their lifetime reduce the effect of degradation due to humidity and moisture. Using the method described in [42] which requires no specialized machine, UV cut film and polymide/Kapton tape are attached on top of the PSC's electrode while avoiding air bubbles from forming. UV cut film was added to protect the perovskite material from the UV light used to cure the Loctite 349 glue which was used to attach a 1-millimeter-thick glass on top of the polymide/Kapton tape. Metal fasteners were also attached on the ITO(negative) and back electrodes (positive) to ensure that there is contact between the electrodes going to the solar cell measuring unit of the satellite and the PSC samples attached to the satellite. During the attachment of the PSCs on the satellite using RTV-S 691, the edges of the cells are also covered with the RTV-S 691 to further protect the sample from the atmospheric environment. A 3-D render of the Perovskite fabricated is shown in Figure 4. The encapsulation materials are also pointed out in the figure.

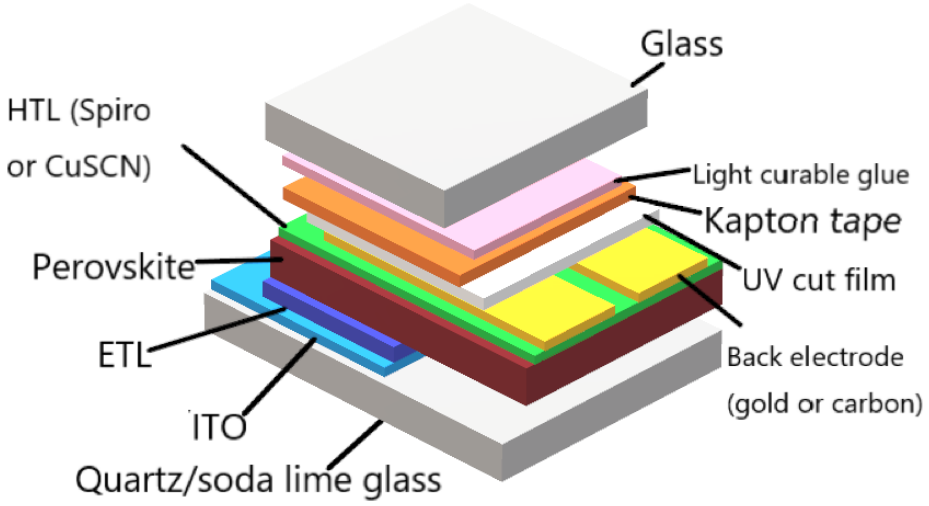

Figure 4 3-D render of the fabricated perovskite layers and encapsulation

The fabricated PSCs have an active area of 0.18 cm^2 shown in a red box in Figure 5. Each square is one sample.

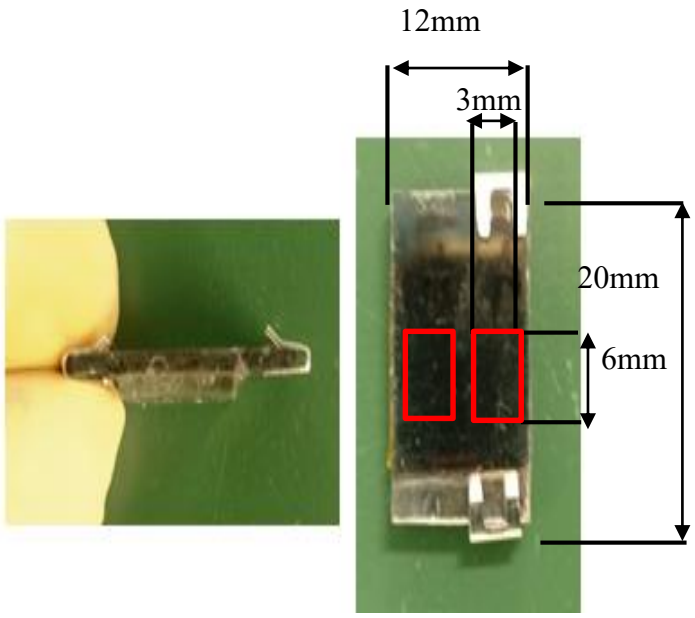

Figure 5 Final encapsulated PSC with active area shown in red box.

3.2 Solar cell characterization

An AM0 solar simulator SML-2K1MV1 Xenon lamp shown in Figure 6 is used to simulate the irradiance from space. A MS-802 pyranometer is used to calibrate the light intensity to approximately 1400 W/m^2 to obtain the reference power conversion efficiency of the fabricated PSCs as shown in Figure 7. The current-voltage measurements are taken using Keithley 2400 source meter connected to a computer running Kickstart application. To maintain a stable temperature on the PSCs being characterized during testing, a fan is used to cool the cell and after each measurement, the cells are covered with an insulator (Styrofoam).

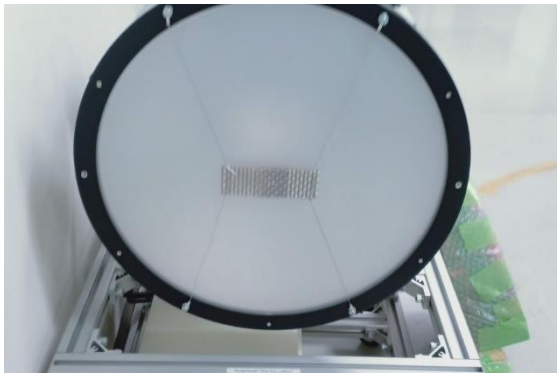

Figure 6 AM0 Xenon lamp sun simulator

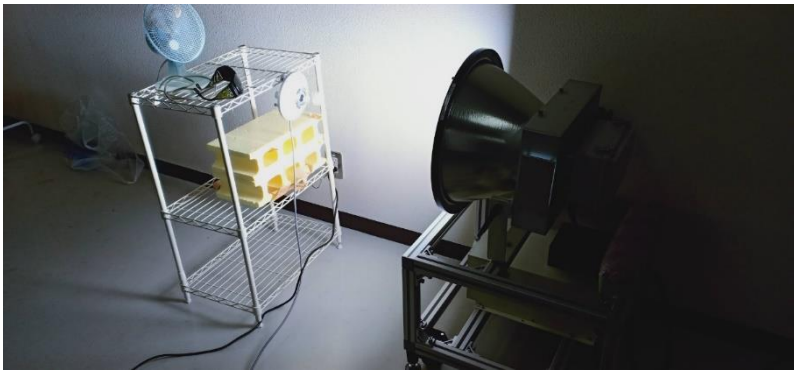

Figure 7 Measurement setup with pyranometer as reference for sun irradiance

To test the effectivity of the encapsulation in protecting the PSCs from moisture and know if the samples would have a chance of still working after long periods of storage prior to flight in space, an accelerated moisture test was performed. The IEC61215 standard which defines the standard for encapsulation and ensure reliability of a solar module for 20 years defines a method done by exposing the solar module to 85% relative humidity at 85°C for 1000 hours where it must retain 80% of its original efficiency to pass. For the accelerated moisture test, a similar environment is employed using a steam chamber to achieve a relative humidity of 70-85% and temperature 65-85°C as shown in Figure 8.

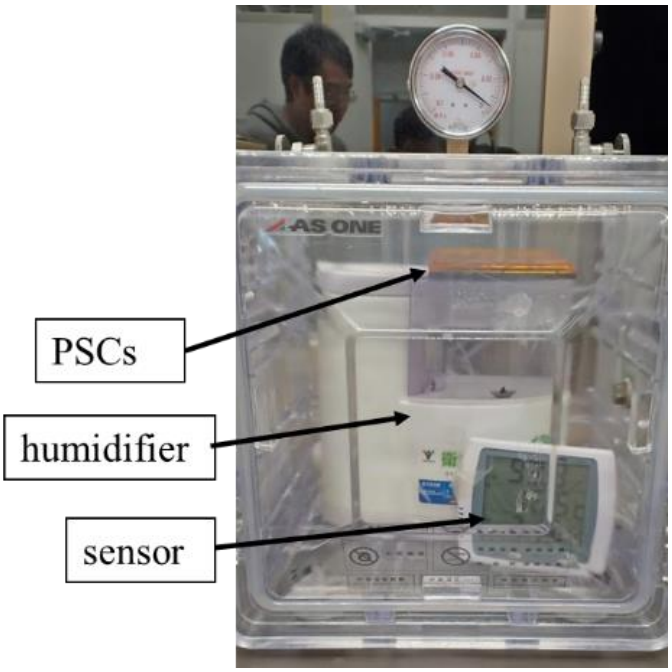

Figure 8 Moisture test setup

The effect of scan direction and scan rate were determined to identify the parameters to be used when measuring the characteristics of the PSC. Literature mentions the hysteresis instability of PSCs which varies depending on the scan direction and scan rate. For the scan direction, forward scanning (from 0V to 1.4V) and back scanning (from 1.4V to 0V) voltage biasing was done. For the scan rate, 765mV/s, 110mV/s and 25mV/s were used to see if the scan rate would have a significant effect on the measured characteristics of the PSCs. The scan rate is varied by changing the delay setting which sets the time a voltage level is used to bias the PSC of the voltage sweep by 0, 0.1 and 0.5 seconds. The current measurement is taken midway of the time that the PSCs are biased. To compare if there is a significant effect between the various parameters, the difference factor, which is computed by computing for the area under the J-V curve and comparing them with other measurements, is used.

A hot air blower was used to increase the temperature of the PSC and determine the temperature coefficient of each type of PSC. The characteristics of the PSCs were measured at

different temperature levels from ambient temperature to 100°C. The change in efficiency and other parameters are plotted to identify how the increased temperature changes the solar cell parameters.

3.2.1 Fabricated Perovskite solar cells performance

An electron microscope image of the layers of the fabricated PSC is shown in Figure 9. The J-V curve of the best sample of each type of PSC is shown in Figure 10 for each type of fabricated PSC and Figure 11 summarizes the parameters of the champion PSCs. Organic HTM has the highest initial PCE, followed by inorganic HTM and finally the HTM free Carbon back electrode PSC. The HTM free PSC also shows lower fill factor compared to the other samples.

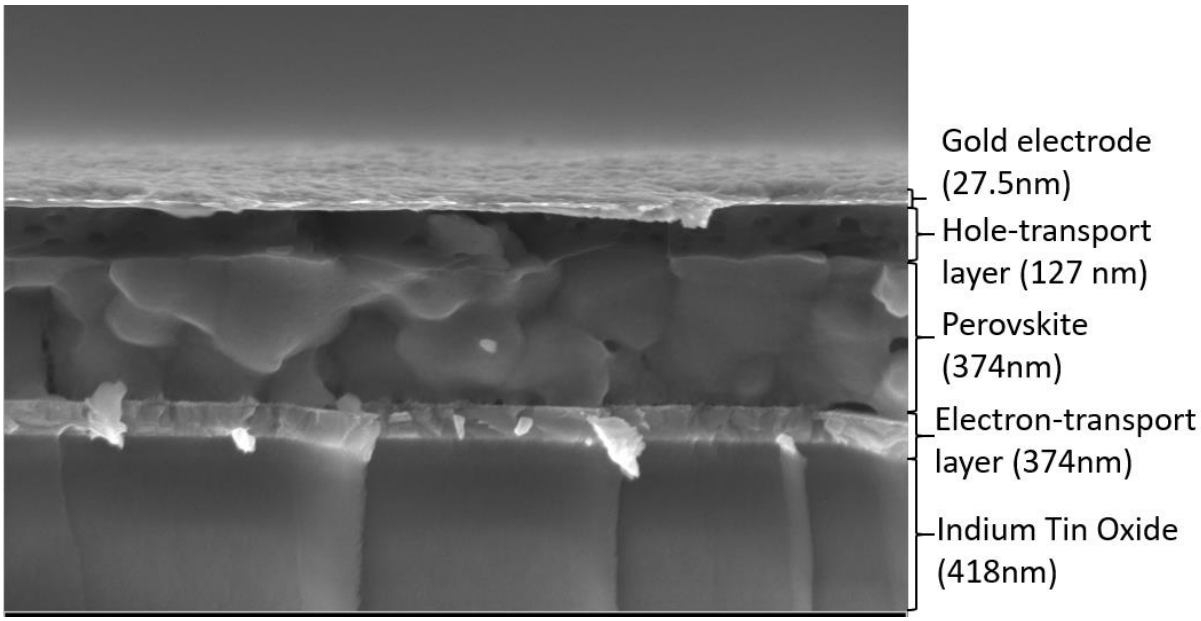

Figure 9 Electron microscope image of the fabricated PSC showing the approximate thickness of each layer, photo courtesy of Shuzhang Yang.

Table 3 Photovoltaic parameters of the Champion PSC for the three types of HTM

HTM Type	Voc(V)	Jsc (mA/cm^2)	FF	PCE (%)
Spiro-OMeTAD	1.07	33.54	0.68	24.28
CuSCN	0.93	32.70	0.66	20.08
Carbon	1.06	31.98	0.36	11.99

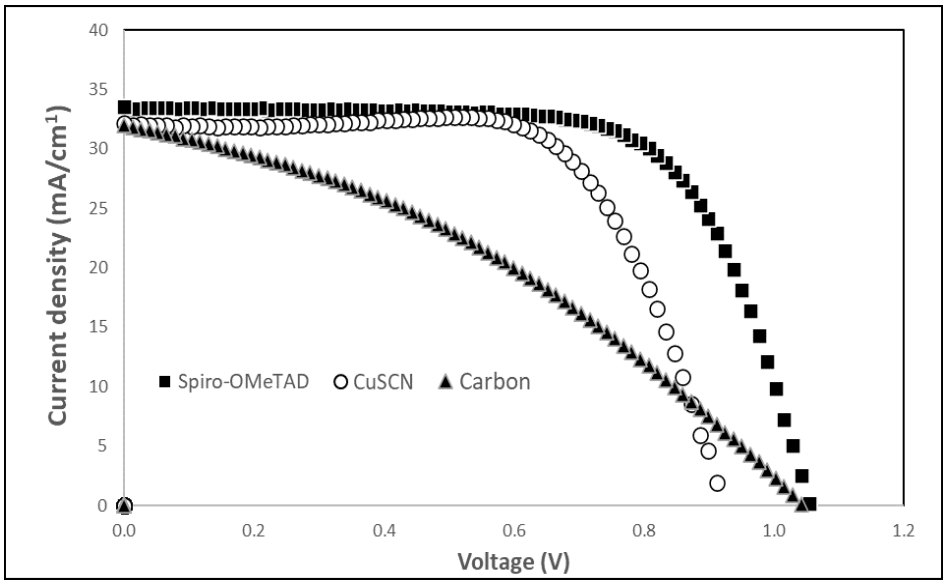

Figure 10 Current density-voltage curves of the champion PSC of the three types of HTM.

A boxplot that shows how the parameters of the samples fabricated are distributed is shown in Figure 11. The boxplot shows how many samples lie in each quartile as represented by the thick bands and thin lines. The first quartile is from the bottom thin line to the thick band, followed by the second quartile from the bottom of the thick band to the middle line which is the median value of the samples. This is followed by the third quartile from the median line to the end of the thick band and finally the fourth quartile from the end of the thick band to the end of the upper thin line. The 'X' marker in the box plot indicates the mean value of the data. A shorter thick band indicates that the values of the samples are not spread apart and the reverse can be inferred if we have a longer thick band [43]. It can be observed that Spiro PSCs have consistent open circuit voltage, while Carbon PSCs have consistent PCE values. The average

PCE of the samples are 12.67, 4.76 and 7.75 for Spiro-OMeTAD, CuSCN and HTM free Carbon back electrode PSCs, respectively. Bad samples are defined as samples with PCE less than three standard deviations (3-σ) from the mean sample since 99.7% of data should be contained within 3 standard deviation from the mean. The computed 3-σ is 3.02 for Spiro,-4.09 for CuSCN and 2.77 for HTM free carbon back electrode samples. From the 24 devices fabricated for simulated space environment tests, 22 samples for Spiro, 23 for CuSCN and 18 samples for Carbon are used for the tests.

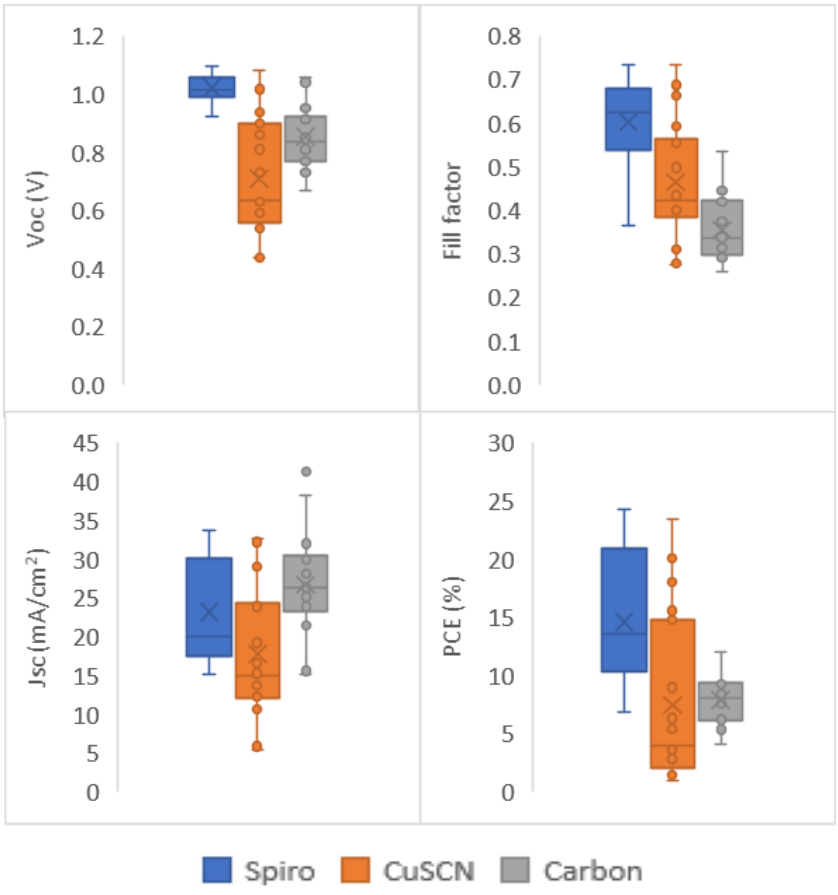

Figure 11 Parameter distribution of fabricated PSCs

3.2.2 Encapsulation and Moisture effect

A difference factor of 10% was computed for the PSC sample before and after encapsulation as shown in Figure 12. This shows that there is some degradation that happened in before and after encapsulation which is probably due to the exposure of the samples to atmospheric condition prior to being encapsulated since the samples are taken out of the glove box during the encapsulation process. Humidity and oxygen might have reacted with the samples degrading the material and resulting to a reduced PCE post-encapsulation.

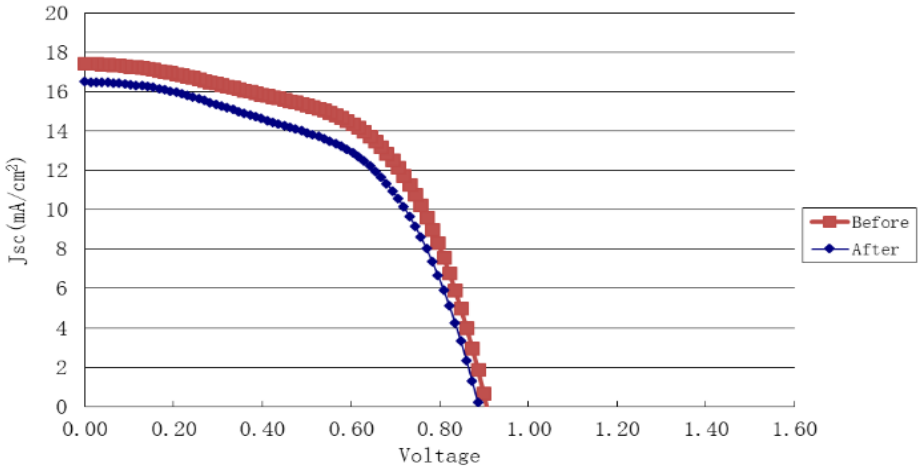

Figure 12 Device efficiency before and after encapsulation

The left image of Figure 13 shows an image of the cells before the moisture test while the middle and right image shows the cells with and without encapsulation after the moisture test. The significant reduction of the active material(black) shows the extensive effect of moisture to the PSC, especially to cells without encapsulation. A comparison of the degradation over time of the PCE of the encapsulated and non-encapsulated cells shown in Figure 14 and Figure 15, respectively, shows that the encapsulation method was somehow able to slow down the degradation of the PSC as indicated by the longer time the PCE is reduced. By scaling the IEC61215 standard that under normal environmental humidity and temperature, Carbon PSCs

would retain its performance for 3.84 years, CuSCN PSCs for approximately 6 months and Spiro PSCs for 2 months. From this results, it can be inferred that the fabricated PSCs would have a chance to still work after waiting for several months in earth prior to the satellites' launch into space.

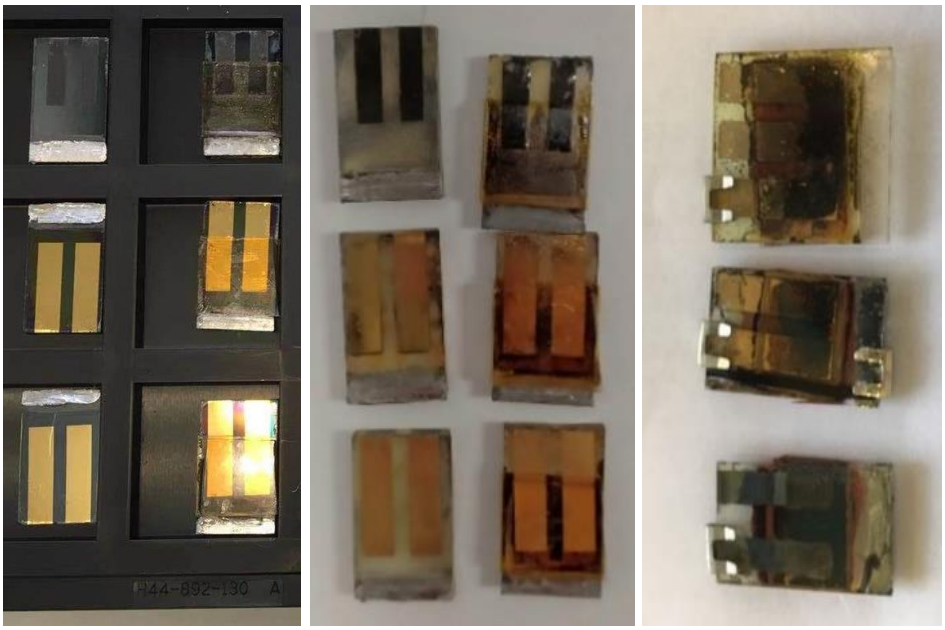

Figure 13 PSC samples (left-right)before moisture test, non-encapsulated cells after moisture test and encapsulated cells after moisture test

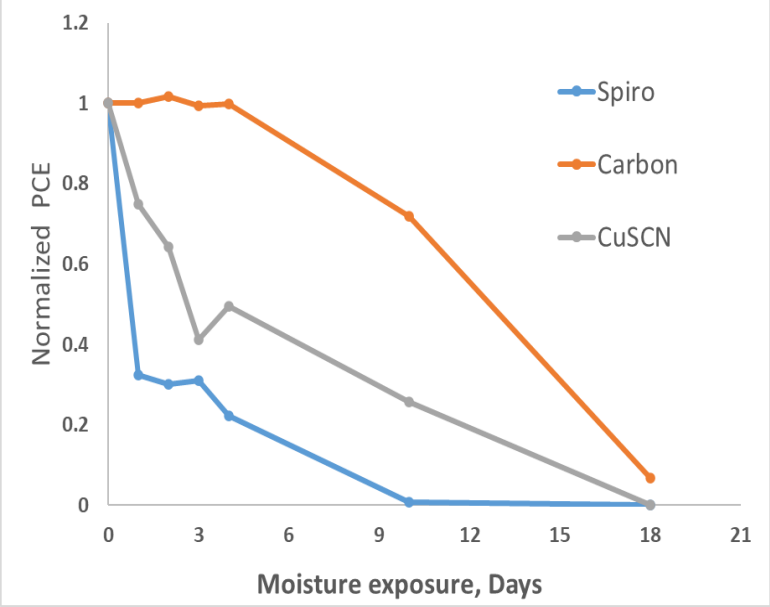

Figure 14 Change in PCE of Non-encapsulated PSCs over time

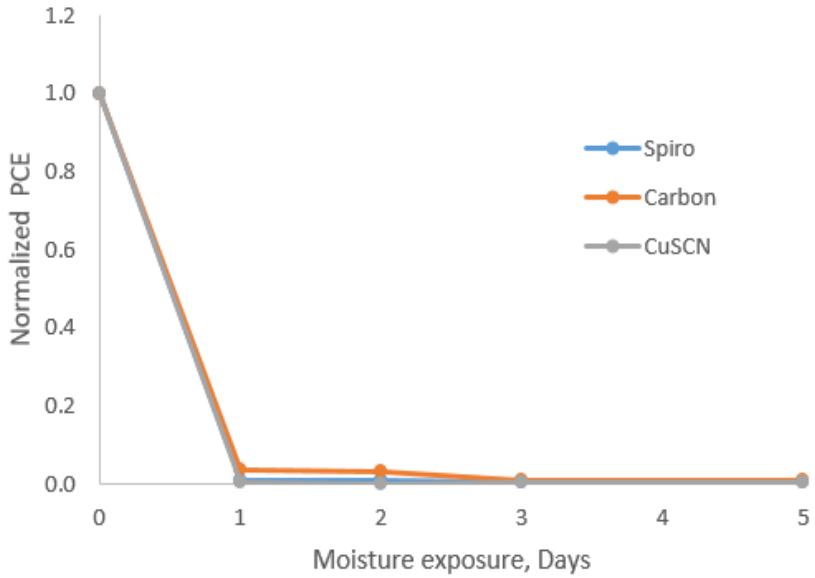

Figure 15 Change in PCE of non-encapsulated PSCs over time

3.2.3 Scan direction and Scan rate

Results on the difference in forward and backward scan direction is shown in Figure 16. The difference factor of Spiro-OMeTAD PSC is 0.93%, 0.69% for CuSCN PSC and 3.87% for the HTM free carbon back electrode PSC. This shows that carbon PSC has the most hysteresis due to scan direction. Since the difference factors are not large, it can be said that the direction of scanning won't have a significant effect on the measured parameters. Hence, backwards scan direction is chosen in measuring the PSCs since scan rate has less effect on backwards measurement and gives a more stable reading at the lower voltage range of the measurement [44].

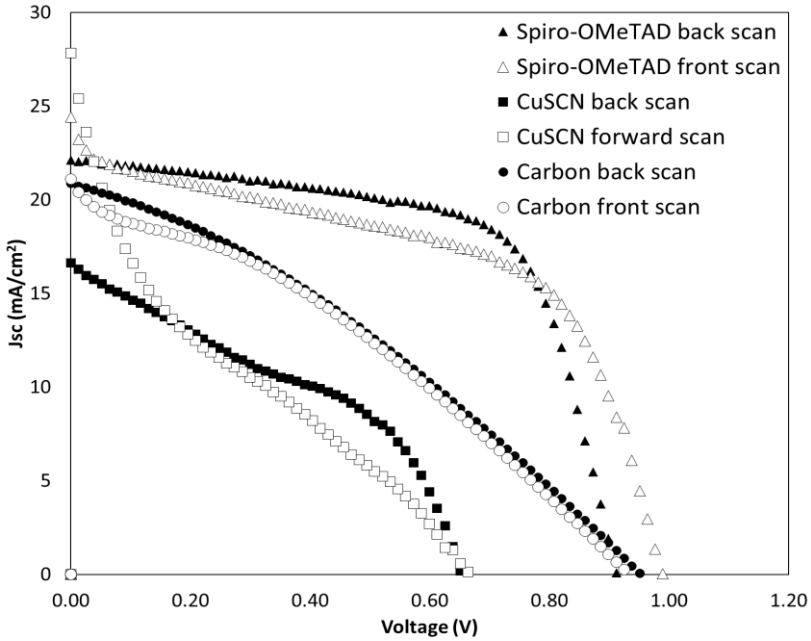

Figure 16 Comparison of PSC samples based on scan

Results of the effect of scan rate are shown in Figure 17. The difference factor of Spiro-OMeTAD is 2.08%, 33.5% for CuSCN PSC and 2.08 for the HTM free Carbon back electrode PSC. From these results, CuSCN has shown to be significantly affected by scan rate, unlike Spiro-OMeTAD and HTM free Carbon back electrode PSCs. Due to the spinning/tumbling of the satellite in orbit, it is preferred to measure the I-V curve as quickly as possible since the irradiance would vary greatly if a long measurement time is employed. From this result, zero (0) second delay or 765mV/s in measurement is used in the scan rate of the PSCs.

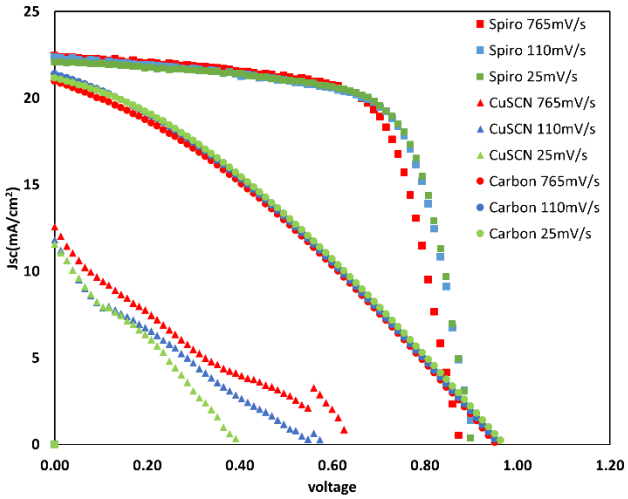

Figure 17 Comparison of PSC samples based on scan rate

3.2.4 Temperature coefficient

The results of the determination of the temperature coefficient of the PSC samples are shown in Figure 18. The normalized temperature coefficient derived are -0.83%/°C for Spiro-OMeTAD, -1.09%/°C for CuSCN and -0.46%/°C for Carbon HTM. Terrestrial monocrystalline solar cells have temperature coefficient of -0.5%/°C [45] while triple junction solar cells have temperature coefficient of -0.09%/°C [46]. Carbon has the best temperature coefficient which shows it is a good material for elevated temperatures. On the other hand, even though Spiro-OMeTAD has the highest initial PCE, its performance is highly reduced in elevated temperature and CuSCN performed worse among the three. Hence, HTM free carbon back electrode PSC has the best temperature stability among the fabricated samples.

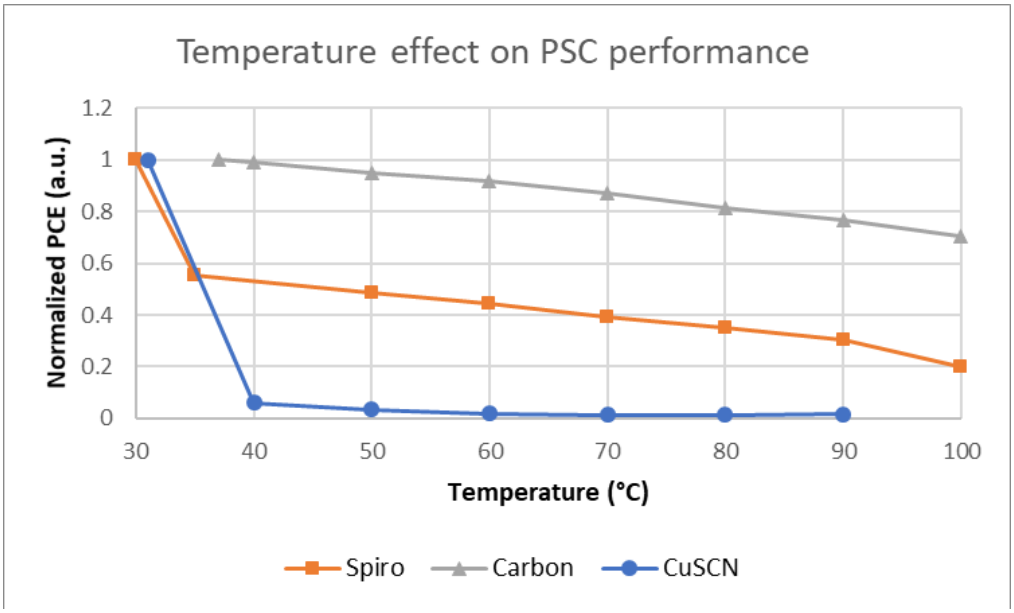

Figure 18 Change in PCE of cells with temperature

Chapter 4: Simulated space environment test

The following simulated space environment test are done to the fabricated PSCs to know how their parameters will change and if they would continue to work under these space environment conditions in low earth orbit:

(1) Thermal cycle

(2) Ultraviolet light (VUV and NUV)

(3) Vibration (during launch)

(4) Vacuum

Due to the limited number of samples, only 2 samples for each type were used for each space environment test. All the space environment tests are done in the Center for Nanosatellite testing (CeNT) and Laboratory of Lean Satellite Enterprises and In-Orbit Experiments (LaSEINE) in Kyushu Institute of Technology, Tobata campus.

4.1 Thermal cycle

A Despatch 900 thermal cycle chamber, shown in Figure 19, was first used to expose the PSCs to temperature cycles from -40 to 85°C for 250 cycles. No temperature soaking was done for each cycle and the solar cell parameters are measured every 50 cycles [47]. In order to isolate the cells from air and moisture during the test, the PSCs were put inside an aluminum pouch with air vacated inside using N_2 gas as shown Figure 20. The pouch is filled and purged of air inside three (3) times before sealing, with only enough space for the thermocouples going to the controller of the chamber.

Figure 19 Despatch 900 thermal chamber

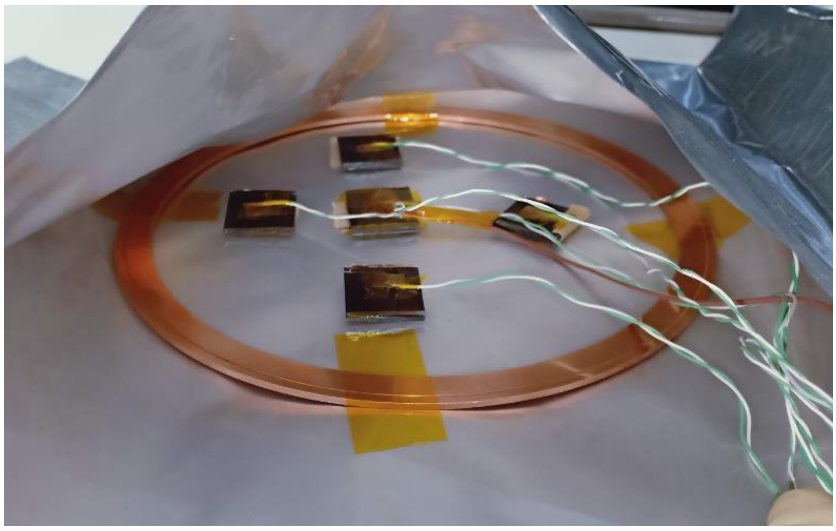

Figure 20 Aluminum pouch to isolate PSCs during thermal cycling

The degradation of the samples as the cycles increase is shown in Figure 21. The efficiency of the PSC has decreased to less than 40% of the original PCE. In Figure 22, it can be observed that the open circuit voltage showed the highest change among the solar cell parameters which indicates that the cycling of temperature has mainly affected the interface between the layers of the PSC. The difference in expansion coefficient of each material led to damage in the interface and decreased the overall PCE and performance of the PSC.

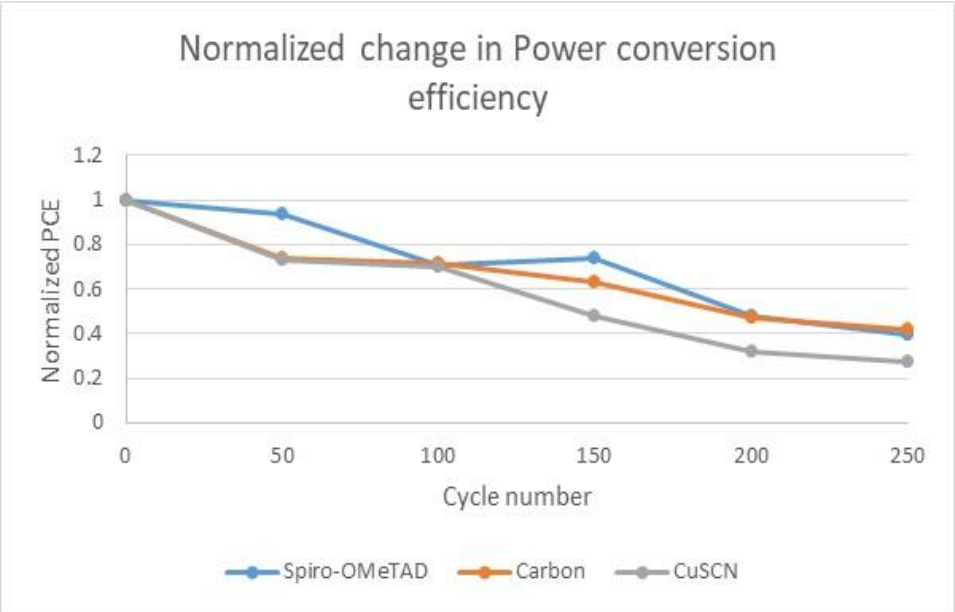

Figure 21 Normalized PCE comparison of three types of PSC after thermal cycling test.

The thermal cycle test was repeated with a narrower range of -20 to 50°C; the minimum and maximum temperature of the external panels based on actual data from the BIRDS-3 and BIRDS-4 satellites. In addition to that, an aged cell was used for the next thermal cycle test which were manufactured on the same batch as the solar cells attached to the BIRDS-4 satellite. For this thermal cycle test, 200 cycles were done with CuSCN HTM Perovskite solar cell. Only this type of PSC was tested because only in-orbit data of CuSCN HTM Perovsktie solar cell was obtained. Shown in Figure 23 is the result of the second thermal cycle test. It can be observed that degradation decreased to only 60% of the initial PCE and an average normalized PCE degradation rate of -0.11% per cycle or -1.65% per day is obtained.

A more accurate thermal cycle test was done by using the average temperature range of the in-orbit data from the satellites which is from -20 to 15°C as shown in Figure 24. For this thermal cycle, the rate of change in temperature was set to 2°C per minute. This was done to see if the rate of change in temperature affects the ground test results. A lower degradation of

less than 90% was observed after 200 cycles and an average normalized PCE degradation rate of -0.07% per cycle or -0.85% per day was obtained as shown in Figure 25.

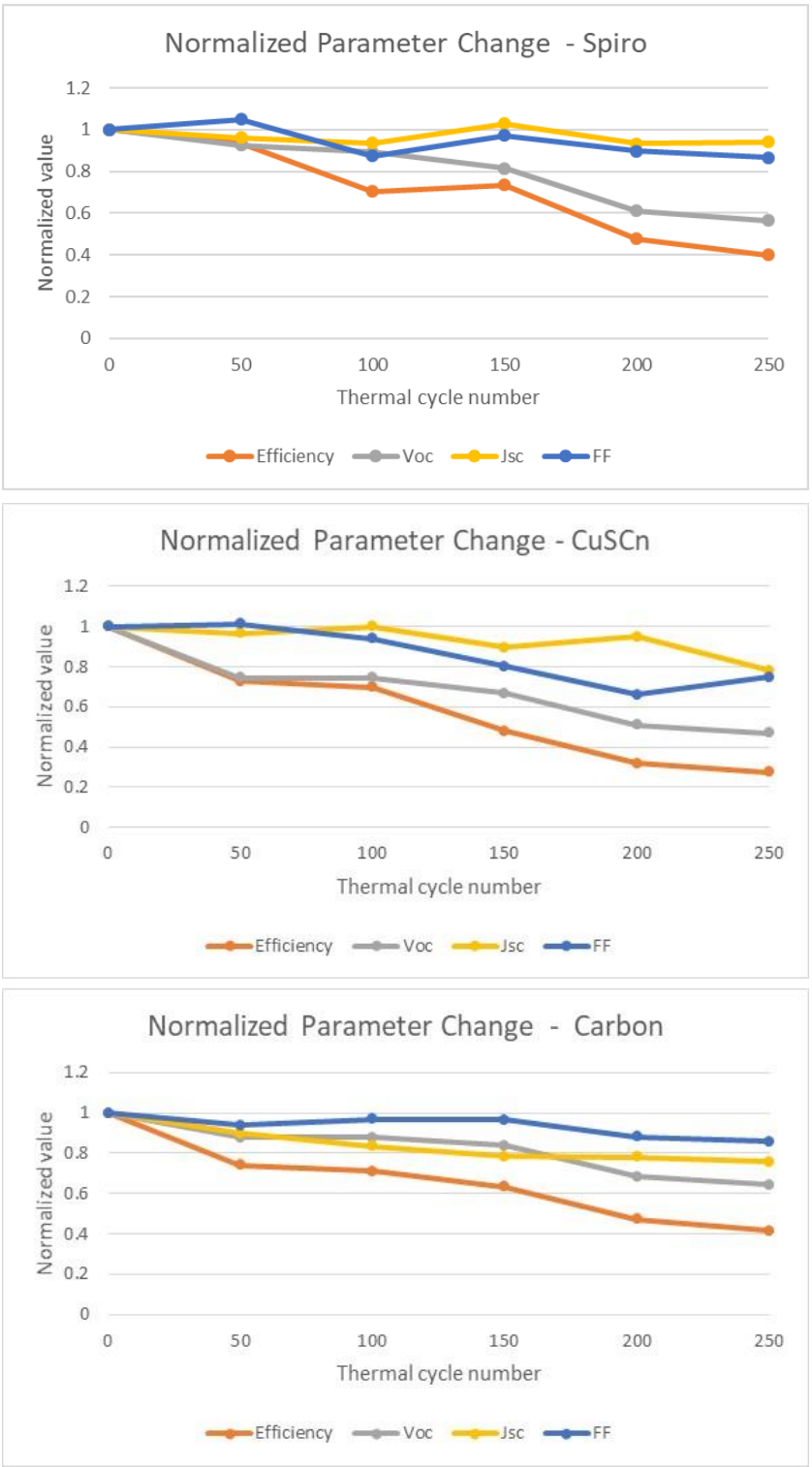

Figure 22 Comparison of the normalized parameters of the three types of PSC after thermal cycling test.

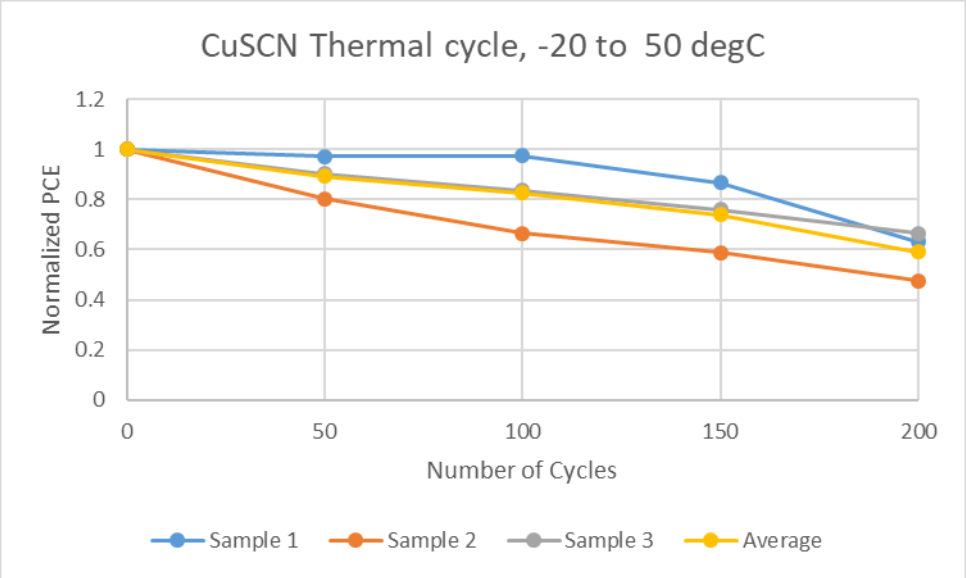

Figure 23 Normalized PCE of aged CuSCN samples after 200 cycles of -20 to 50°C thermal cycling

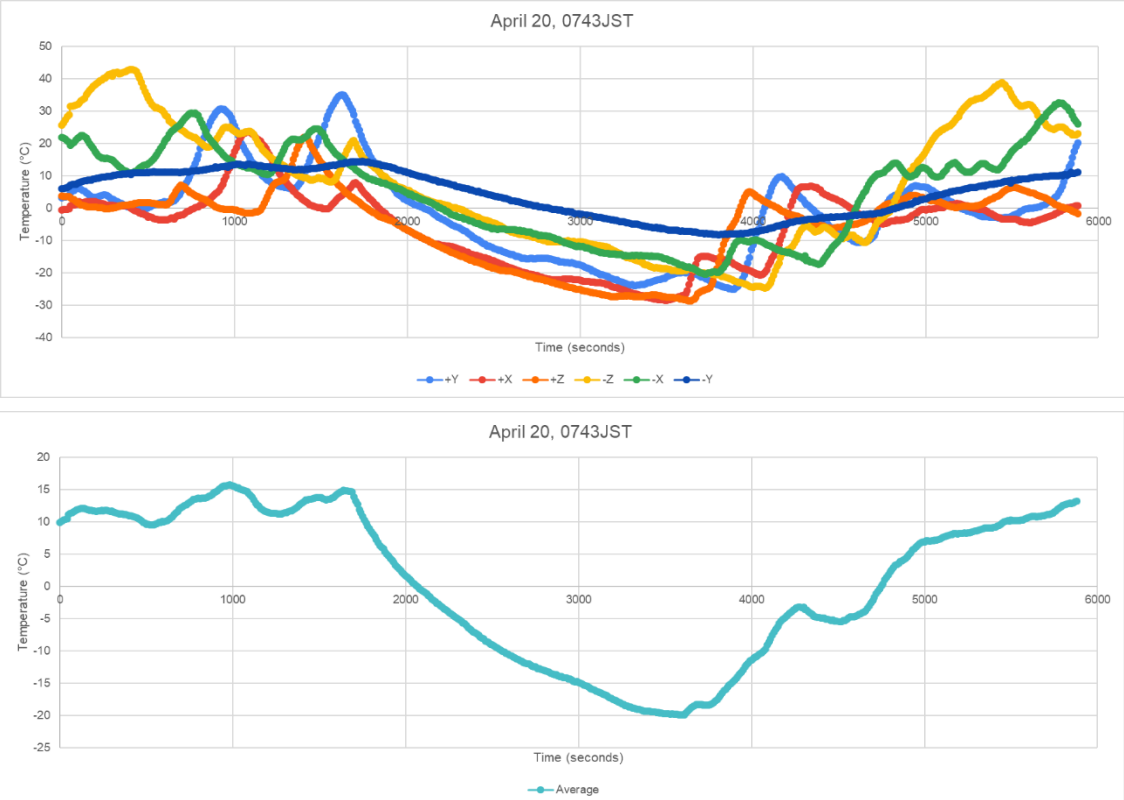

Figure 24 (a) Temperature of external panels of BIRDS-4 satellite Tsuru and (b) average value of external panel temperature

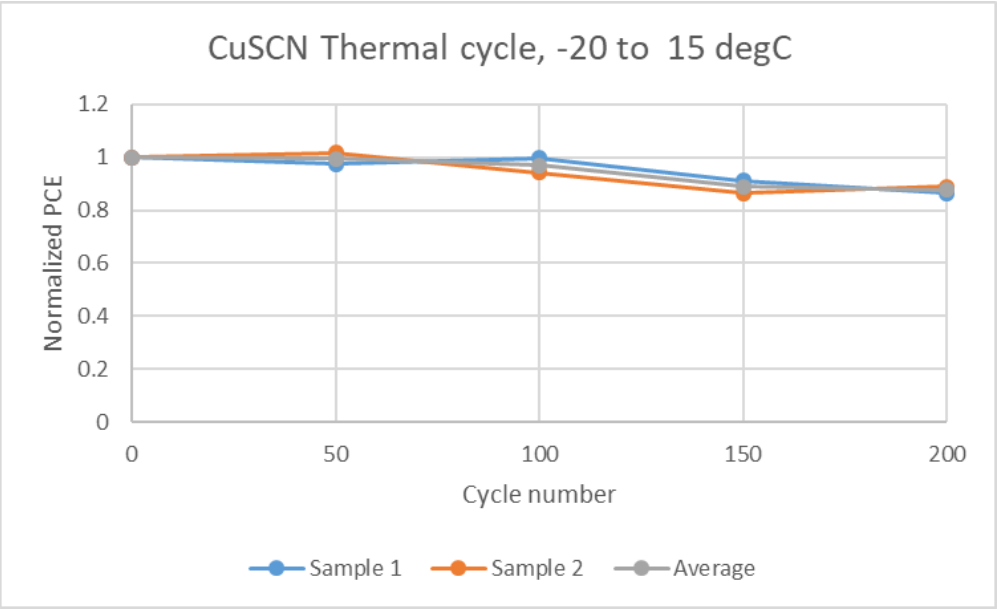

Figure 25 Normalized PCE of CuSCN HTM PSC after 200 cycles of -20 to 15°C at a rate of 35 minutes per cycle.

A final thermal cycle test was done, which followed the average rate of change of temperature in space and allow a more accurate simulation of the environment. One cycle is set to 90 minutes at a temperature range of -20 to 15°C. When measurement was being done after the 150th cycle, the cells seemed to have broken down and no valid data was recorded.

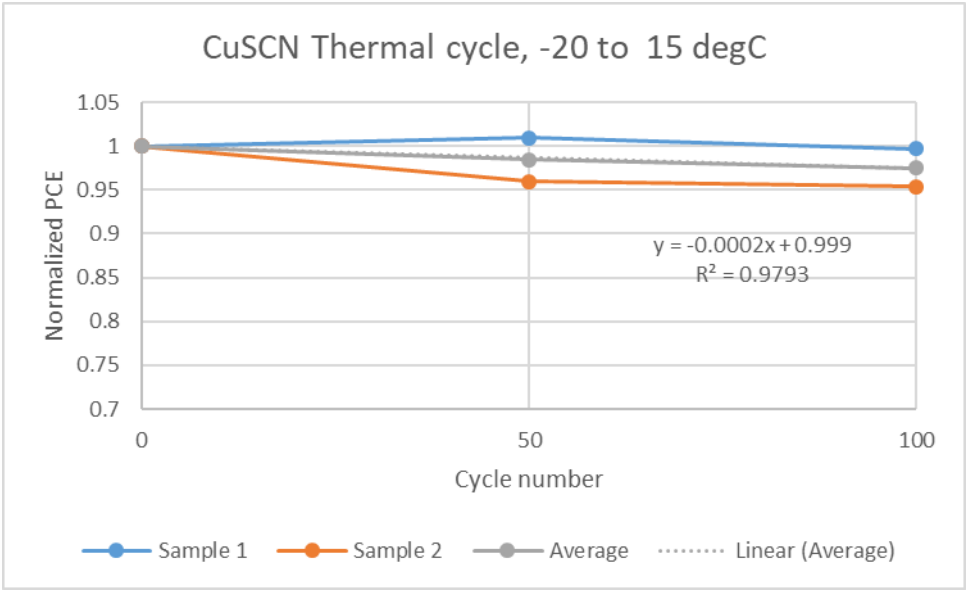

Figure 26 Normalized PCE of CuSCN HTM after 100 cycles of -20 to 15°C at a rate of 90 minutes per cycle

Results showed less degradation rate at -0.02% per cycle or -0.30% per day as shown in Figure 26.

In general, it can be observed how thermal cycling significantly affects the performance of the PSCs. Literature suggests that the difference in thermal expansion coefficient of the different layers of the PSC leads to breakdown of the interfaces, resulting to reduction in overall power conversion efficiency. Shown in Table 4 is a comparison of the thermal expansion coefficient of the PSC, indicating that Perovskite material has ten times more expansion coefficient which results to cracks and damage at the interfaces [48] [49] [50] [51] [52] [53].

Table 4 Thermal coexpansion coefficent of different PSC layer materials

Material	CTE (10^{-6} m/°C)
Soda lime glass	9
ITO	7.2
SnO_2 (ETM)	4
Perovskite	~50-60
Spiro-OMeTAD (HTM)	4.6
CuSCN (HTM)	-20
Carbon (graphite)	2-6

4.2 Ultraviolet radiation

The fabricated PSCs use SnO_2 as the electron transport layer and a UV cut film is attached to the glass surface facing the sun to ensure that UV radiation will not degrade the PSCs. The transmittance of the UV cut film was measured and as shown in Figure 27, it cuts almost 90% of UV light above 370nm wavelength.

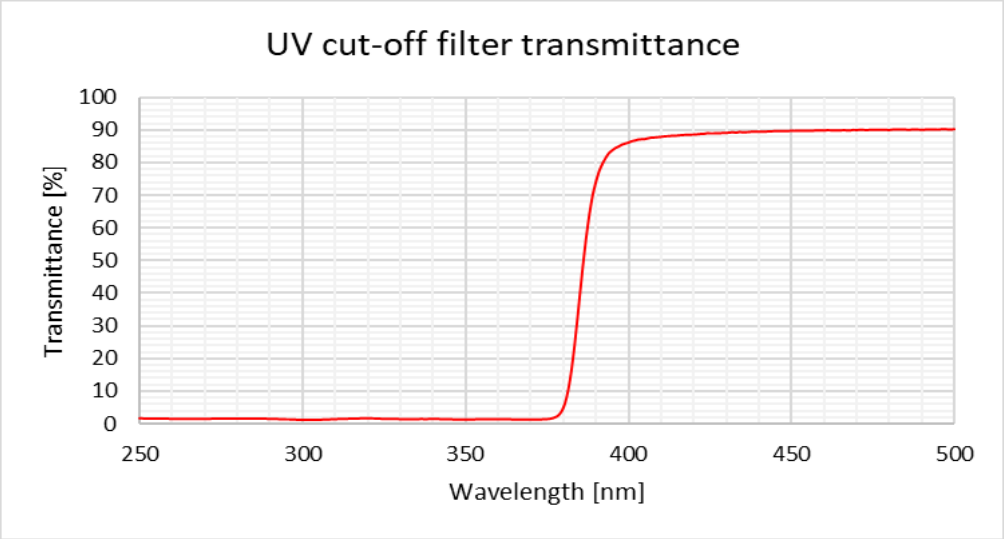

Figure 27 Attached UV cut film transmittance spectrum

The fabricated PSCs were exposed to Near UV (NUV) using a Hamamatsu L2273 Xenon(Xe) lamp and Vacuum UV (VUV) using a Hamamatsu L12542 Deuterium(D2) lamp. A different set of PSCs were used for each type of UV radiation. Figure 28 shows the UV spectral radiation in space and the spectral radiation of the UV lamps used in the test. Two PSC samples are tested for each type of HTM on both the NUV and the VUV light. Two PSC samples for each type of HTM were also put inside the chamber but are not exposed to the UV radiation. These will serve as control samples and basis of comparison if UV radiation did affect the performance of PSCs or the vacuum and thermal environment were the only factors for the change in performance.

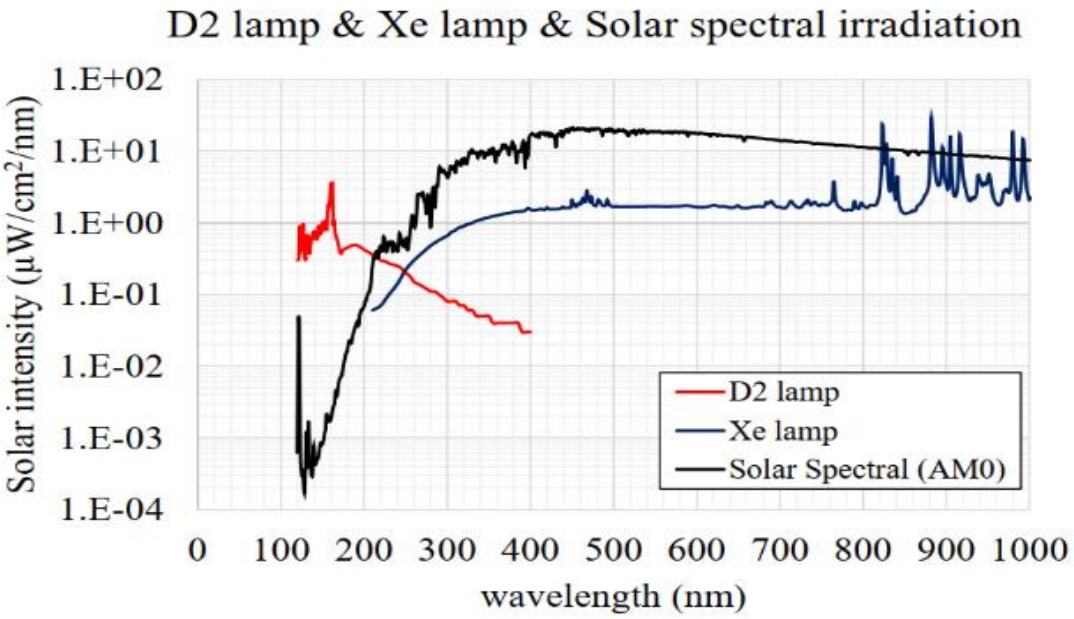

Figure 28 Spectral response of Deuterium (D2) and Xenon lamp vis-à-vis AM0 Solar spectrum.

The NUV test chamber exposed the PSCs to a light intensity of 23 mW/cm^2 at a vacuum condition of 3.5 x 10^{-3} Pa. The high intensity resulted to an increase in temperature of the exposed cells up to 80°C during the test. The normal sun intensity in space at 200-400 nm is about 10.85 mW/cm^2 only. The PSCs were exposed to an equivalent of 450 sun hours which translates to one month of exposure in low earth orbit. The VUV chamber exposed the PSCs to an average solar intensity of 106 μW/cm^2 at a temperature of -40°C and vacuum condition of 1.6 x10^{-4} Pa. The normal sun intensity in space at 120-200 nm is about 10.44 μW/cm^2. Similar to the NUV test, the PSCs are exposed to an equivalent of one-month exposure to VUV radiation. The VUV test was repeated twice using same samples. In the first test, the UV cut film were attached and for the second test, they were removed to see if the UV cut film had an effect in preventing the degradation of PSCs. The setup for the VUV and NUV radiation test are shown in Figure 29.

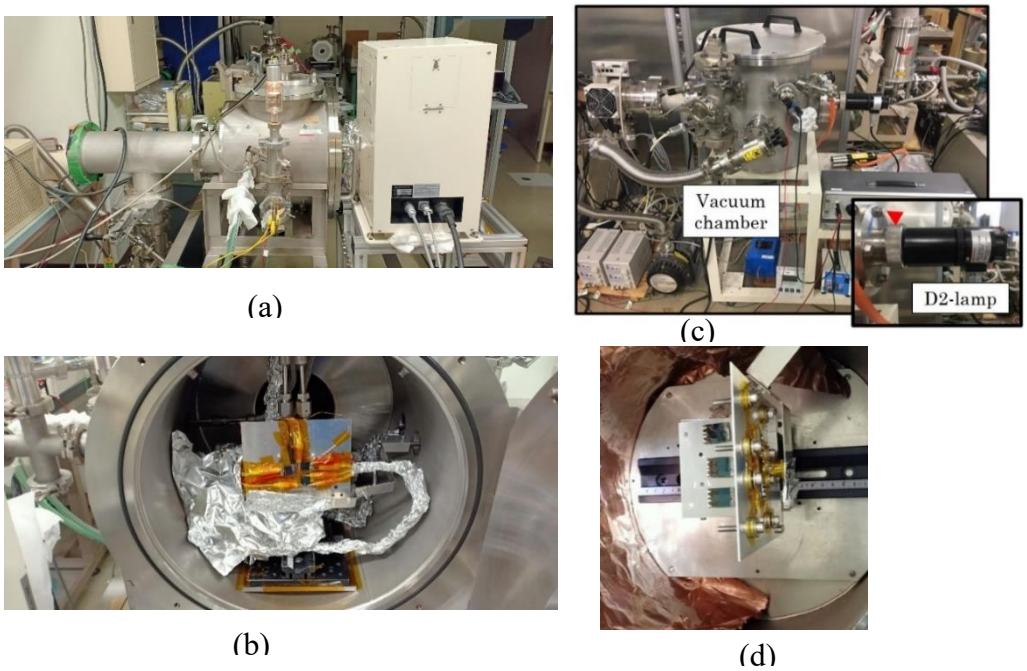

Figure 29 UV chambers used in the test (a) Near UV chamber utilizing Xenon lamp (b) PSC samples inside the NUV chamber (c) Vacuum UV chamber utilizing Deuterium lamp (d) PSC inside the VUV chamber

The results of the change in PCE during the 1-month equivalent in-orbit NUV test is shown in Figure 30. Both the PSCs with organic and inorganic HTM degraded quickly while the HTM free carbon back electrode PSC has shown better long term stability under the high UV intensity and temperature (~80°C). After conducting the test inside the chamber, the cell

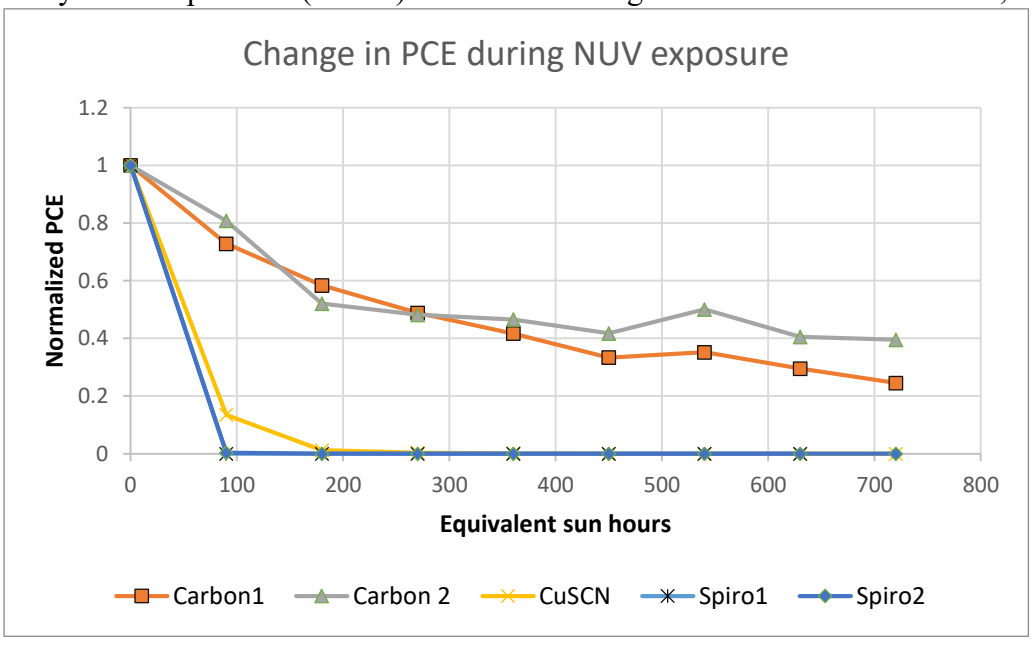

Figure 30 Change in PCE over time during NUV test

parameters are measured again and the results shown in Figure 31 indicates that PSCs using Organic HTM Spiro-OMeTAD and Inorganic HTM CuSCN stopped working after being exposed to continuous NUV and high temperature compared to the control samples placed inside the chamber but not exposed to the NUV radiation. The HTM free Carbon continued to function after the NUV test but with reduce efficiency compared to its initial efficiency. Although it cannot be concluded if NUV or the increased temperature caused the degradation in performance, we know from the thermal coefficient characterization that PSCs don't work well in increased temperature. This test also showed that PSC using carbon as back electrode have better temperature stability due to the increased thickness it has compared to the vacuum deposited gold, which provides better insulation of the material from the environment.

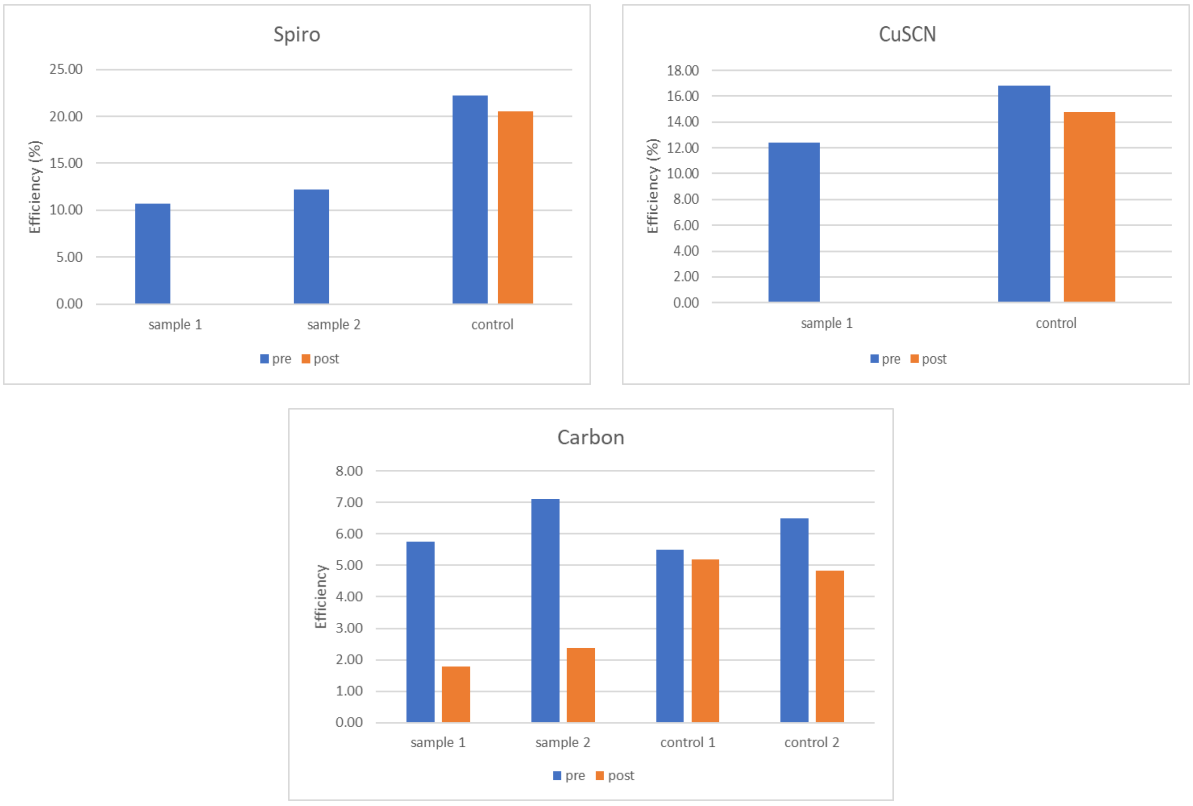

Figure 31 Comparison of PCE of PSCs with different HTM pre- and post- NUV radiation

The results of the first VUV test, where samples have a UV filter attached are shown in Figure 32. Both the exposed and unexposed cells degraded during the test and the amount of change is almost the same for the cells that were exposed and those that were not exposed. Since the amount of change for the samples exposed to VUV and the control samples are relatively the same, it can be said that with the UV filter attached, the VUV radiation did not affect the PSCs and degradation is due to the temperature and vacuum environment.

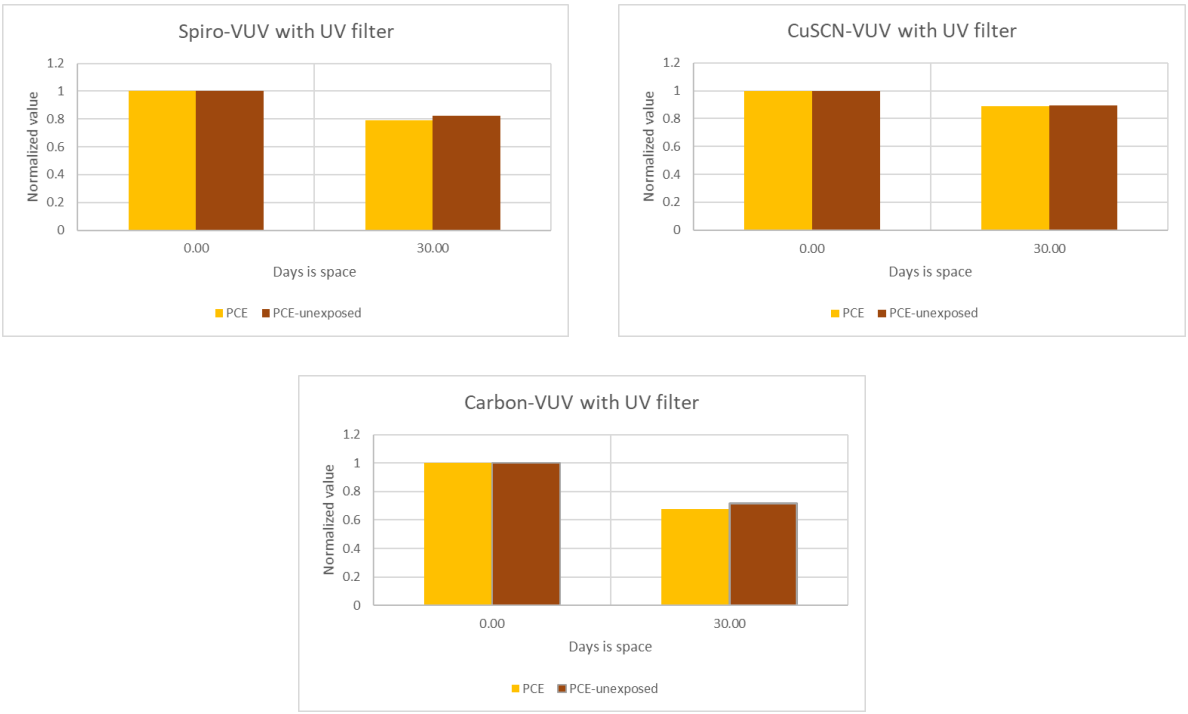

Figure 32 Comparison between the change in PCE between the PSCs exposed and not exposed to VUV radiation.

The VUV test is repeated on the same cells used in the previous test without the UV cut filter to see if the filter had a significant effect in the performance of the cells. The J-V curves shown in Figure 33 indicates that only the HTM free carbon PSC degraded, while other cells showed no degradation and a slight increase in performance. A study by Roghabadi et al [48] explained that UV treatment could cause modifications of the bulk properties of PSCs and its energy equilibrium at the interfaces by passivating the surface and grain boundary defects. A similar explanation could also explain why the parameters remained the same for the samples

without UV cut filter. It is difficult to conclude if VUV is the cause of degradation of the HTM free Carbon PSC with a small sample space. Future research could further investigate this phenomenon to arrive at a better conclusion of the results of this experiment.

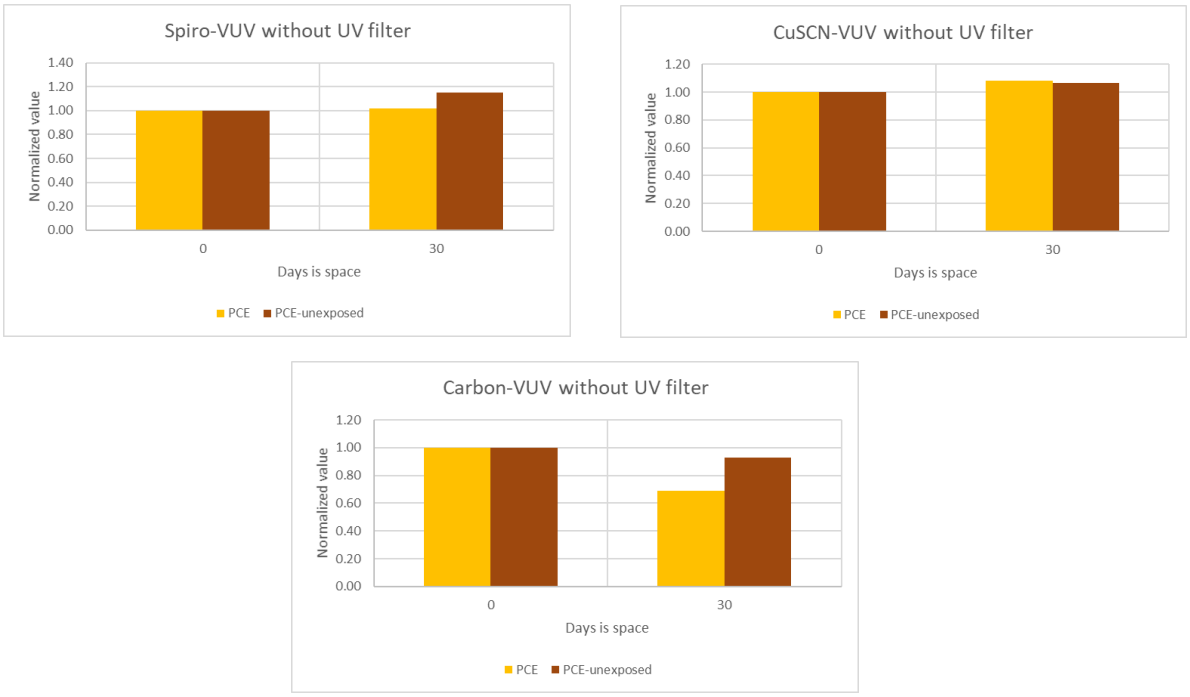

Figure 33 Comparison between the change in PCE between PSCs without UV cut filter

4.3 Vibration

The satellites would experience high levels of acceleration during launch which could damage components or lead to removal from surfaces where they are attached to. As such, the PSCs attached to the satellite undergo acceptance test level of vibration based on the power spectral density (PSD) of common launchers to ISS: SpaceX, Cygnus and HTV. Shown in Figure 34 is the Power spectral density of the aforementioned rockets and the Power density envelope used during the vibration test with root mean square value of 6.79G RMS. The solar cells attached to the satellites were exposed to this level of random vibration to see if there would be damage to the cells or if they would be detached from the satellite.

(a)

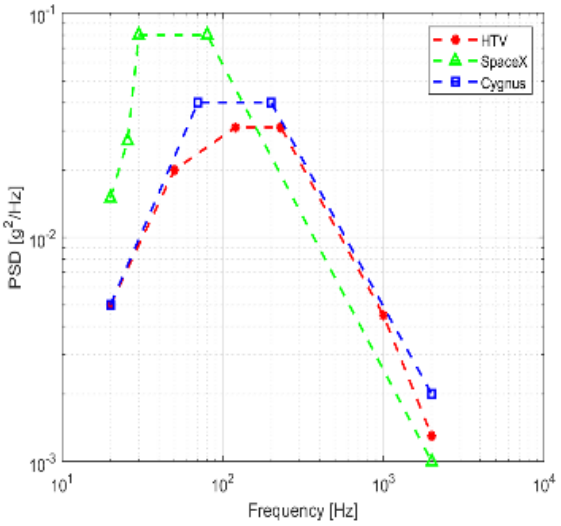

(b)

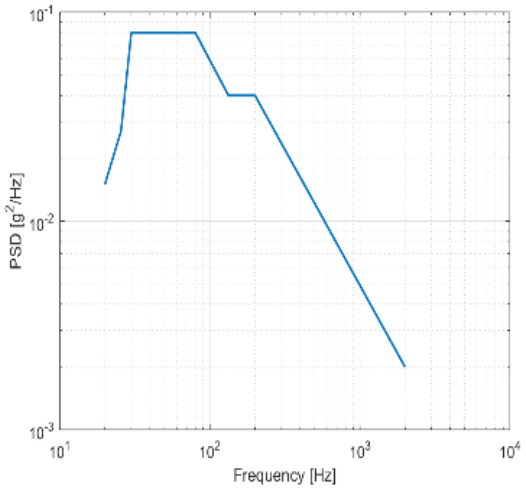

Figure 34 (a) Random vibration PSD of HTV, SpaceX and Cygnus rockets (b) envelope of the PSD profiles of the three launchers.

Figure 35 shows the flight model of the BIRDS4 satellites inside the pod that is connected to the vibration test machine. The PSCs and the PSC attachment method was able to pass the acceptance test random vibration levels from the envelope of the vibration profiles of common ISS launch vehicles. Upon optical inspection, no cracks or chipped particles from the PSC samples were observed after the vibration test and it remained steadily attached to the surface of the satellite. Figure 36 shows a comparison between a carbon PSC before and after

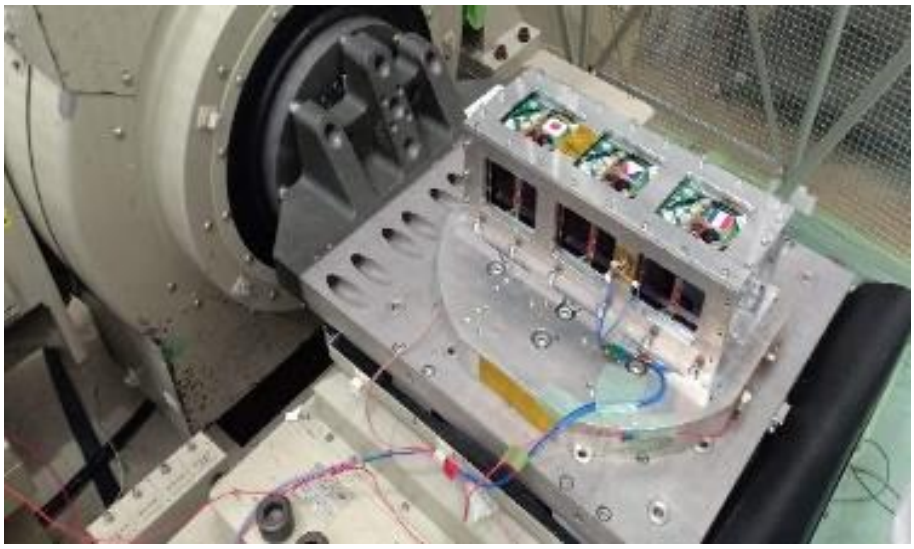

Figure 35 Vibration test machine and satellites inside pod for vibration test

vibration test. A slight discrepancy of the results is pointed as a result of human errors and inaccuracies during measurement. A change in distance between light source and test sample of approximately 2-3cm or an angle change of 10-15 degrees from the normal incident angle show a change in measured current. The change in distance and angle is a result of the cell being placed vertically from a platform which is moved from its location based on the measured irradiance of the pyranometer being used as reference as shown in Figure 7. Utmost care was taken to maintain consistent placement of cells during measurement, but changes in distance and angle of the cell could still happen as a result of human error.

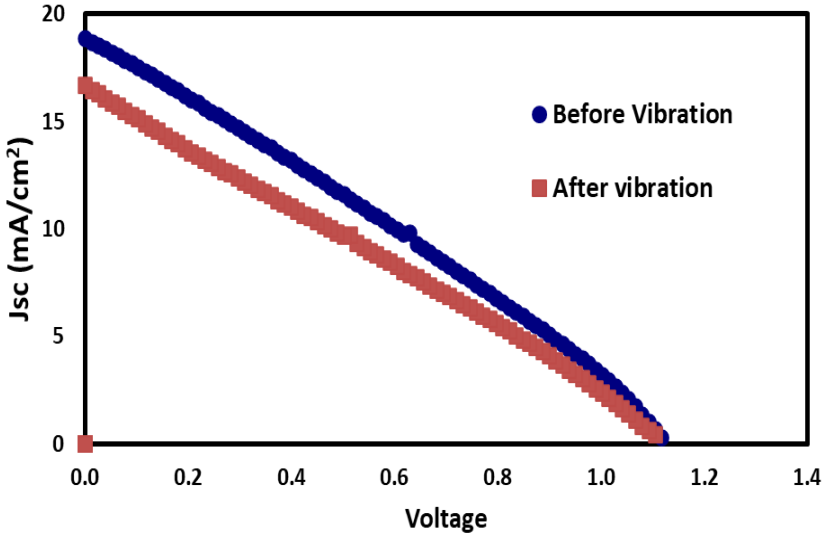

Figure 36 Comparison of J-V performance of PSC before and after vibration test.

4.4 Vacuum

The high vacuum condition in space could result in outgassing of materials that could affect the electronics or optics of other payloads of a satellite. Hence, Vacuum testing was done in a chamber shown in Figure 37 by putting PSC devices inside a vacuum chamber at 4 x 10^{-5} Pa for 200 hours. The samples are weighed using AMPUT APTP-453 digital scale with 0.01g resolution and characterized before and after vacuum test to see if outgassing occurred. The

cells are also inspected optically for any cracks, chips or discoloration. Another set of PSCs were left in atmospheric environment under 30-40% relative humidity at 23°C to serve as control group and reference if vacuum environment has significant effect on the solar cells.

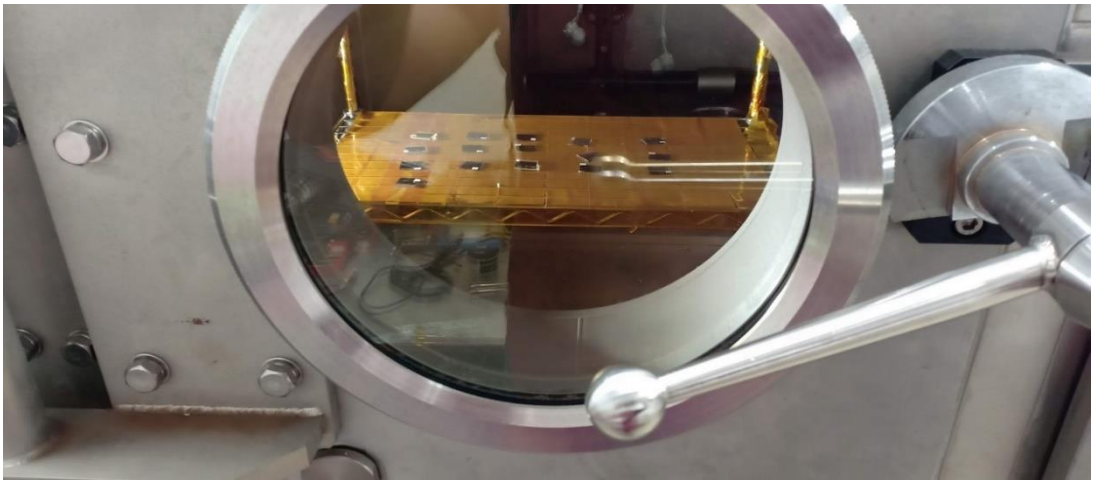

Figure 37 PSCs inside the vacuum chamber

For the outgassing of the encapsulated samples, visual inspection of the samples for any cracks, chips and discoloration showed no change before and after the vacuum test. A 0.01 gram change in weight was observed in some samples while the rest of the samples did not change their weight at all as shown in Figure 38.

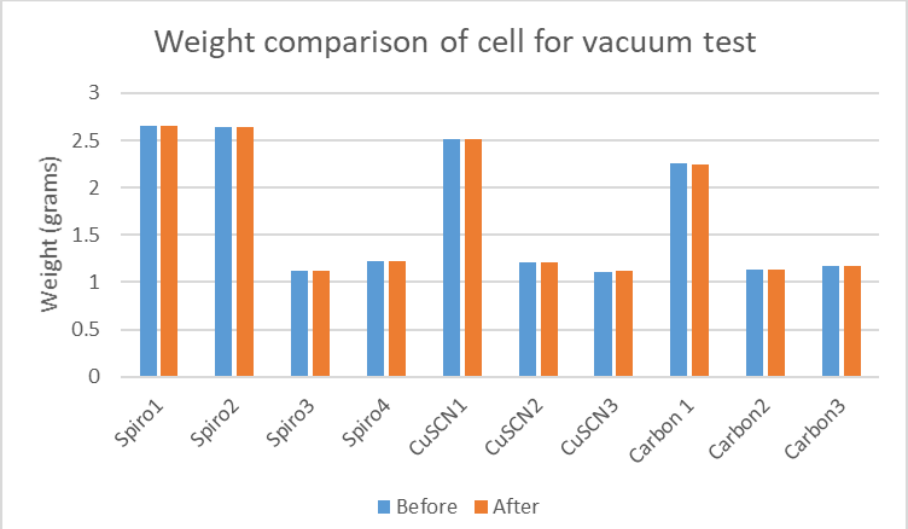

Figure 38 Weight comparison before and after vacuum test of the encapsulated and non-encapsulated samples

Comparison of the performance of the samples exposed in vacuum and normal atmospheric conditions after 200 hours are shown in Figure 39. It is expected that vacuum would reduce the effect of atmospheric environment but the results show that there is still some change in the performance of the cell. Spiro-OMeTAD samples displayed 25% and 35% reduction in initial PCE, while the CuSCN sample only changed by 0.4% from its initial PCE and HTM free carbon PSC samples showed 5% and 25% reduction. Comparing with the change in initial PCE for samples outside the vacuum chamber, where a 69% and 35% change was observed in the Spiro-OMeTAD sample, 4% and 12% change in CuSCN and a 12% and 2% change in HTM free carbon PSC, it can be concluded that vacuum environment is better suited for the encapsulated PSCs. Another thing to highlight is the lower change in initial PCE for

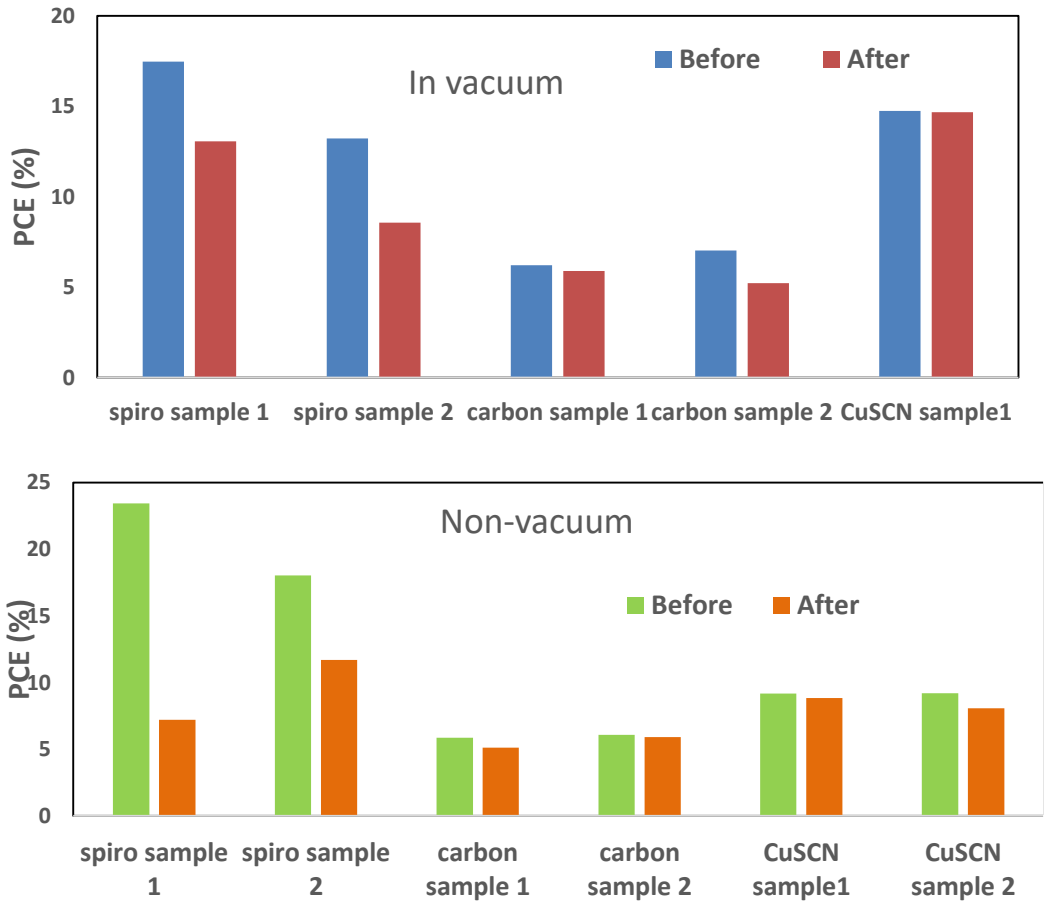

Figure 39 Comparison on the change in PCE of samples exposed to vacuum and not exposed to vacuum

CuSCN and HTM free carbon PSC, compared to organic HTM PSC. Ion migration is pointed by Jiang et al [35] for the continued degradation of PSCs even in vacuum environment.

The vacuum test was repeated with aged PSCs manufactured the same time as PSCs attached to the satellites. For this test, only CuSCN samples were used again and the same samples as those used in thermal cycle test. The PSCs were exposed to $4x10^{-4}$ Pa using the thermal vacuum chamber shown in Figure 40. The cells were exposed for 200 hours and the performance of the cells were measured every ~100 hours.

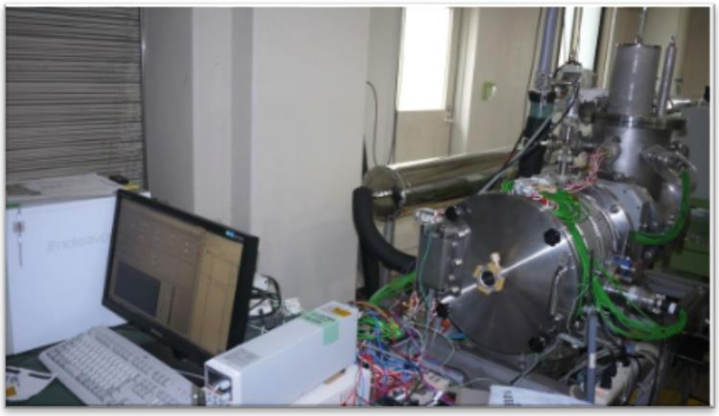

Figure 40 Vacuum chamber used in the experiment with aged perovskite solar cells

The results of the vacuum test are shown Figure 41. It can be observed that the normalized change in PCE is lower in the aged cells compared to the fresh cells tested in the earlier section with an average normalized PCE degradation of 0.009% per hour. This indicates that with the cells ageing and finish reacting, it reaches a stable condition that prevents further reaction with the environment.

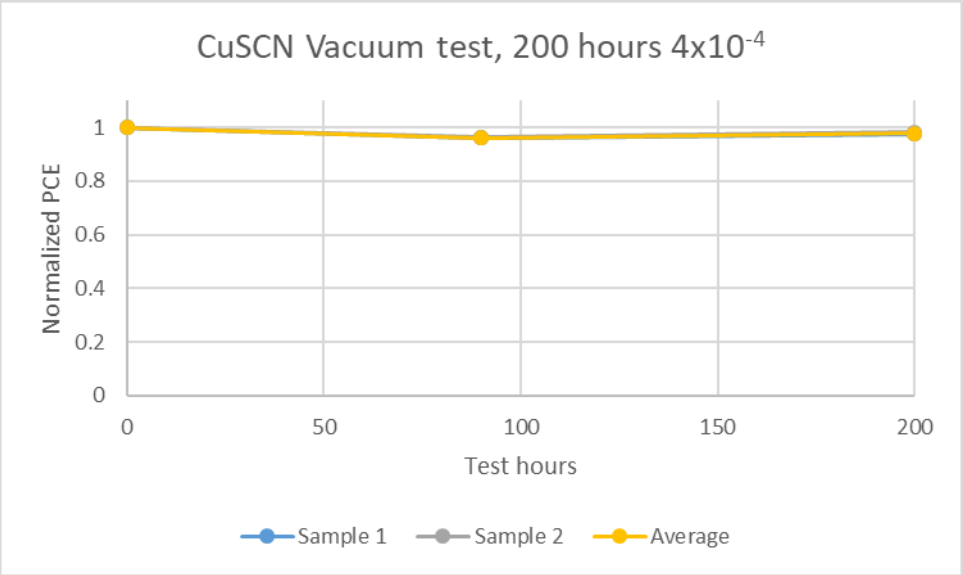

Figure 41 Vacuum test results on Aged perovskite solar cells

Chapter 5: Perovskite solar cell mission and In-orbit data

Through the fourth iteration of the Joint Global Multi-Nation Birds Project or BIRDS-4 project, graduate students representing Japan, Philippines and Paraguay built three (3) identical Cube satellites. Two PSC samples were attached in each satellite with the Philippine satellite carrying the PSC with Spiro-OMeTAD HTM, Paraguay satellite carrying PSC the HTM free Carbon back electrode, and Japan satellite carrying the PSC with CuSCN HTM. A solar cell measuring circuit is one of the payloads inside each BIRDS-4 satellite which functions similar to a source meter by biasing the PSC and measuring the current output. A TMP36FSZ IC is used as a temperature sensor on the surface where the PSC is attached and a SFH 2430 photodiode serves as a sun angle sensor to be used as reference for the irradiance the PSC receives for each I-V curve measurement. The collected current, voltage, temperature and sun angle data are processed by a PIC16F1789 microcontroller and stored inside a 1 gigabit flash memory chip. The block diagram of the system is shown in Figure 42.

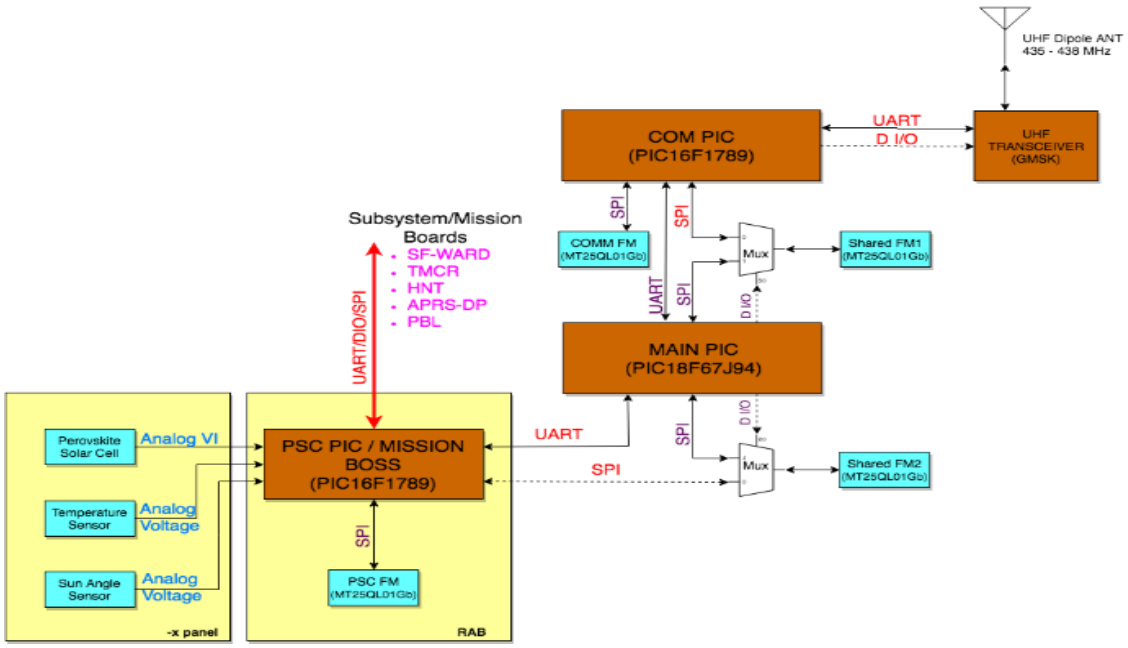

Figure 42 Block diagram of Perovskite Solar Cell Measurement Unit.

The solar cell measuring unit implements a buffer circuit and current sensor as shown in Figure 43. Bias voltage is changed from 1.4V to 0V for 110 steps. This sweep takes approximately 12 seconds and 5 seconds to save all the measured data into a flash memory. The system waits for a specific time dictated by the ground station command sent to the satellite before taking the next I-V curve measurement. A minimum of one (1) minute of interval can be done in between measurements. The data processed by the PIC microcontroller are converted from 4-byte float format to a 2-byte integer format to reduce the memory necessary to complete an I-V curve measurement for the 2 samples attached to the satellite. The float is converted to integer by multiplying the float value by 10,000 for the voltage value and by 100 for the current, temperature and solar intensity. A total of 880 bytes is stored for each set of measurement for the 2 cells attached, equivalent to 11 packets of data needed to be downloaded to reconstruct the I-V curve and determine the PSC parameters.

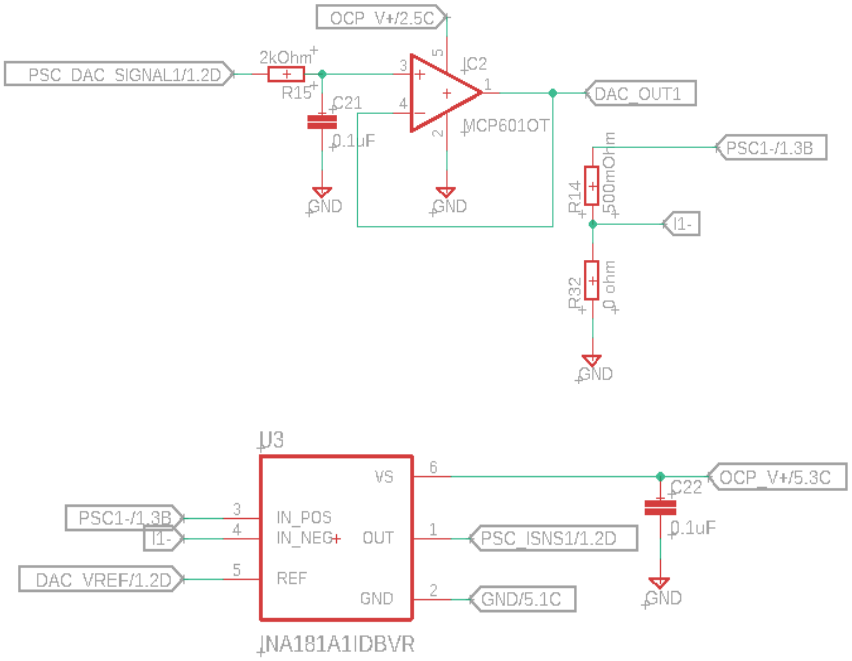

Figure 43 Circuit diagram of the Perovskite solar cell measurement unit

5.1 Solar cell measuring unit

The solar measuring unit is part of the Rear Access Board (RAB) of the BIRDS4 satellite. It contains the PIC microcontroller, buffer circuit and current sensing circuit as shown in Figure 44. The board is connected to the Perovskite solar cells, temperature sensor and photodiode sun angle sensor through the 50-pin connector. The Perovskite solar cell, temperature sensor and the photodiode sun angle sensor are placed in the –Y panel of the satellite, along with the UHF, VHF and GPS antennas as shown in Figure 45.

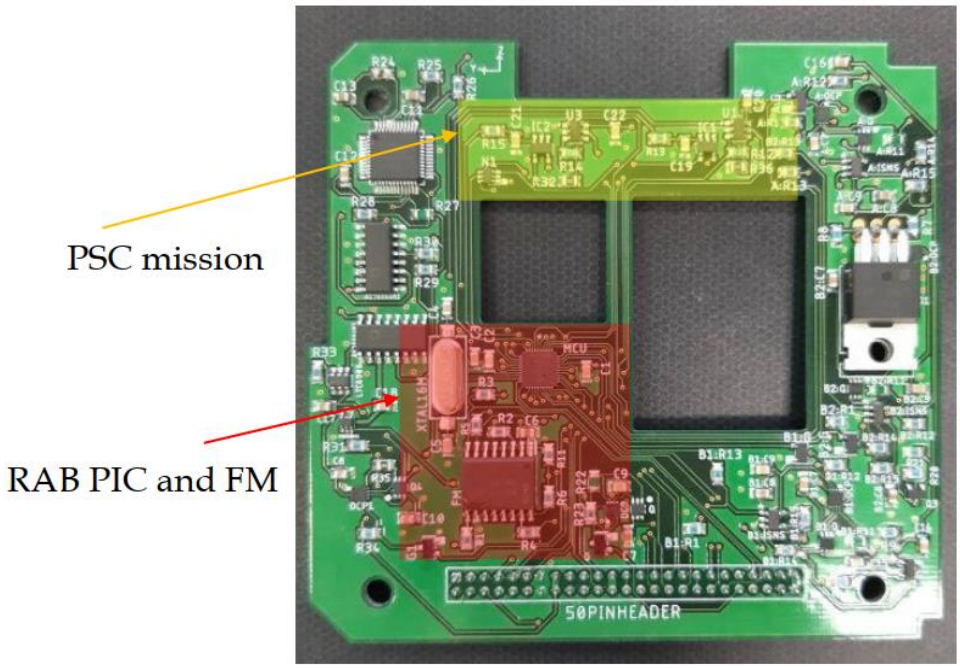

Figure 44 Birds-4 Rear access board containing the solar cell measuring unit

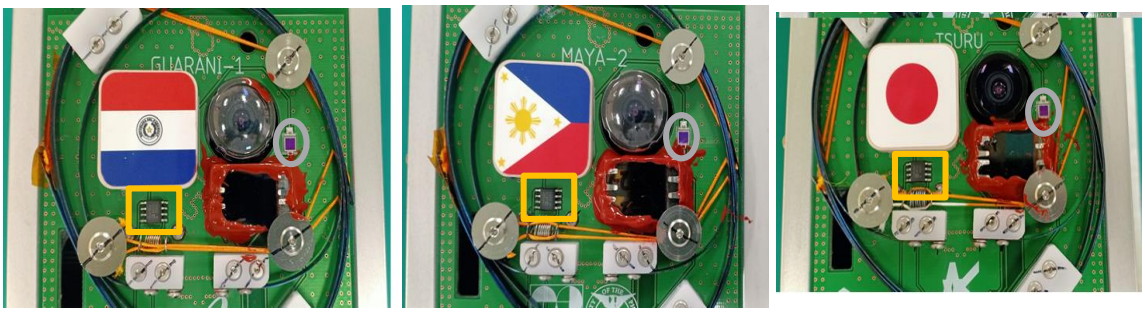

Figure 45 PSC samples attached to each satellite of BIRDS-4 with photodiode (circled) and temperature sensors (squared).

5.1.1 Solar cell measuring unit calibration

Calibration of the on-board solar measuring unit was done by comparing the output of the source meter and the solar measuring unit. Figure 46 shows the results after calibrating the solar cell measuring unit to closely match the measurement done by the source meter. The Keithley source meter has a measurement resolution of 1pA/100nV or 10μA/V while the source meter has an average resolution of 12mA/V due to the lower resolution of the analog-to-digital converter and current sensor used in the solar cell measuring unit. A slight offset in open circuit voltage was observed as a result in a slight increase in temperature of the cell during the experiment. The change per unit temperature in the Voc ranges from 0.0027 – 0.0091 V/°C.

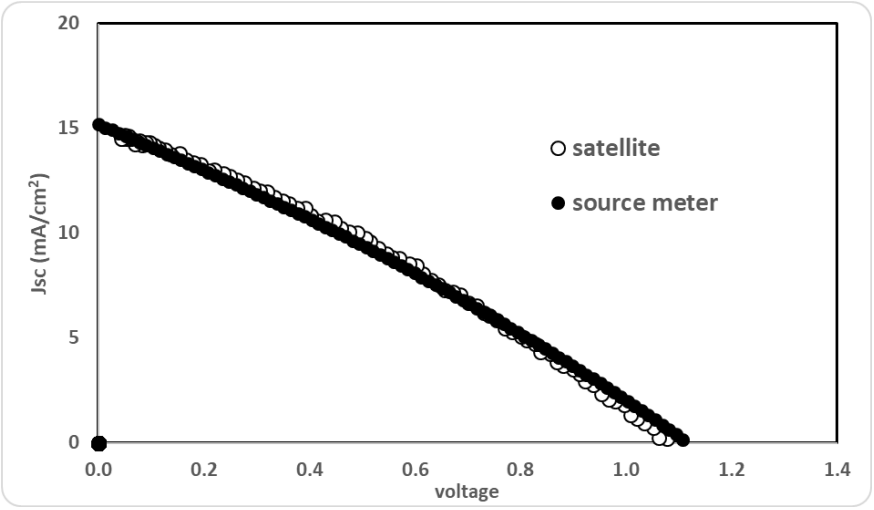

Figure 46 Comparison between source meter and satellite PSC measurement unit.

5.1.2 Sun angle sensor calibration

Sun angle sensor was also done by varying the incident angle of light and plotting the output of the photodiode. Results of the photodiode calibration is shown in Figure 47. Using the sensor output, we can derive the irradiance assuming an AM0 irradiance of 1367W/m^2 and multiplying it by the cosine of the sun angle relative to the normal vector of the solar cell surface. This irradiance value is then used in computing for PCE of the solar cells in space.

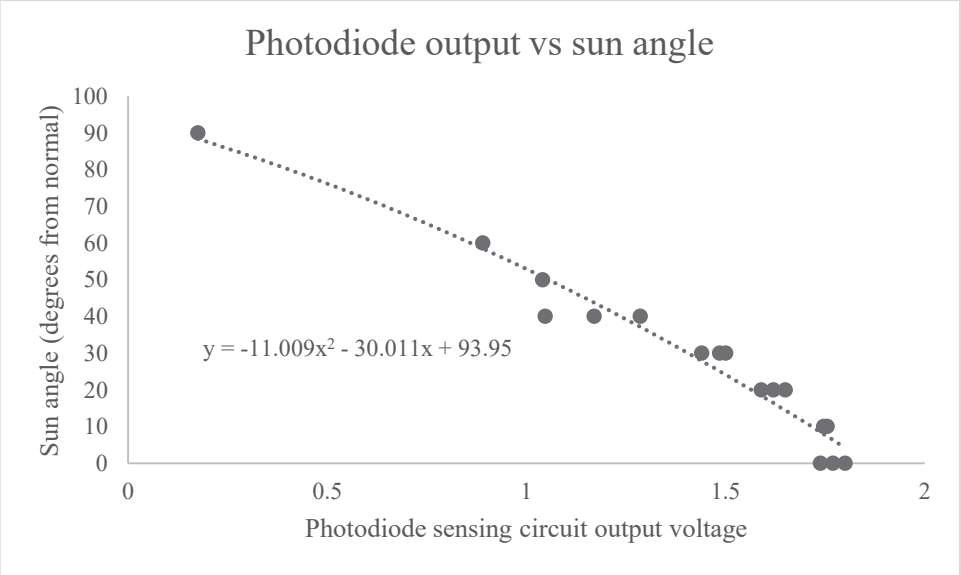

Figure 47 Photodiode sun angle sensor calibration results

5.2 Pre-flight testing

Prior to the hand-over and delivery of the BIRDS4 satellites for its launch to the ISS, the perovskite solar cell mission is simulated by sending a command using the ground station, to the satellite flight models where the final PSCs are attached. After running the mission for several measurements, the data saved were downloaded and processed. A J-V curve plot of the fresh PSC and the downloaded pre-flight mission simulation are shown in Figure 48. The figure shows that all the PSCs attached have degraded in their performance 1 month after their

attachment, with the Spiro-OMeTAD having the worst degradation. The results agree with the moisture test where the organic PSC also degraded the most, although it was not expected to degrade this much under normal atmospheric environment. Hence, it was decided to replace the Spiro-OMeTAD sample and the HTM free Carbon PSCs but unfortunately, there wasn't enough time to once again compare the performance of the freshly fabricated samples and the cells when they were attached to the satellite. This result reinforces the need for better encapsulating method for future satellite missions that would utilize PSCs to make sure that the cells are still in good working condition when sent to space.

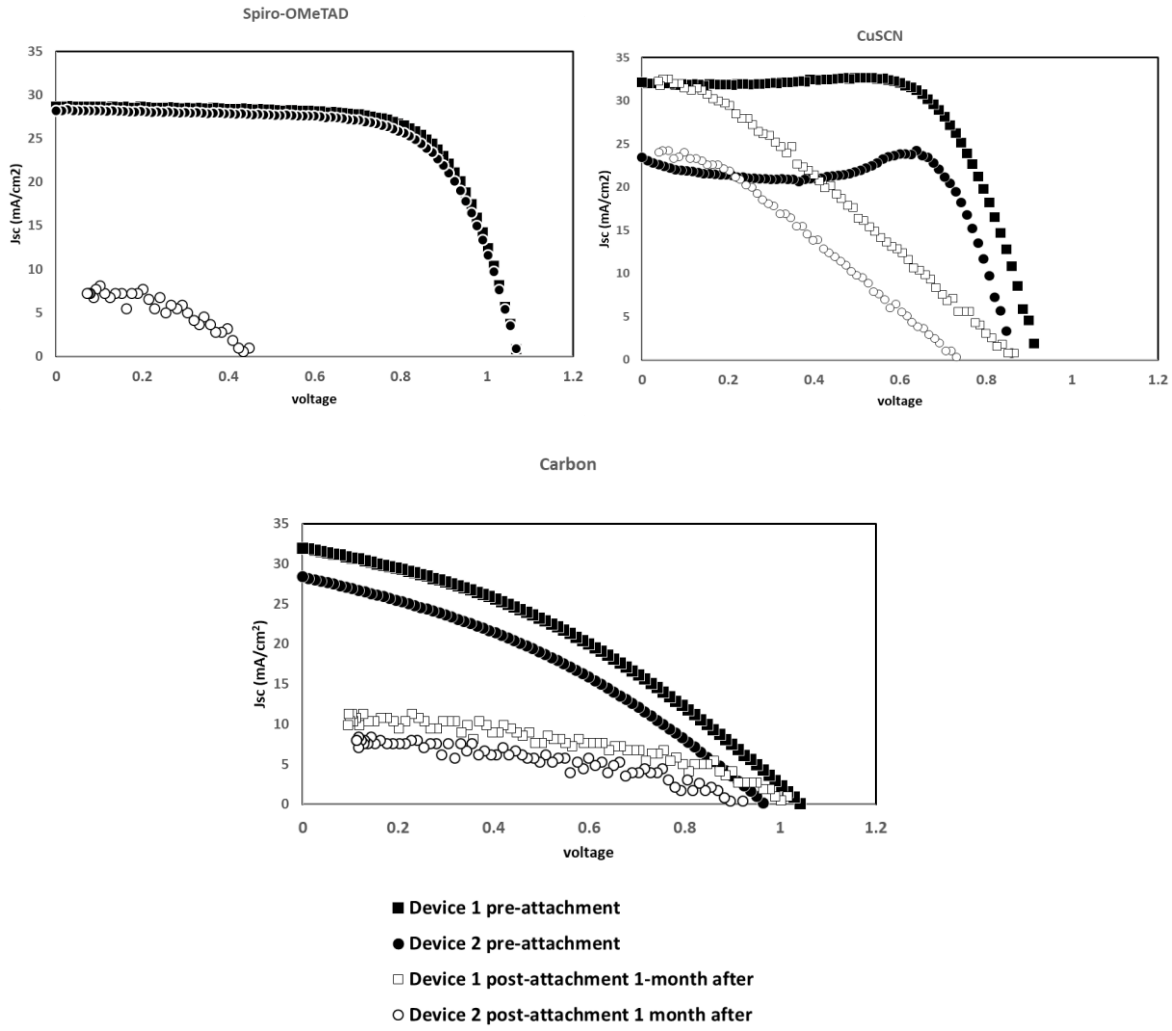

Figure 48 Comparison between devices attached to the BIRDS-4 satellites before attachment and 1-month after attachment

5.3 In-orbit space data

The BIRDS-4 satellites are deployed into space on March 14, 2021. Shown in Figure 49 is an image taken by Astronaut Soichi during the deployment of the BIRDS-4 CubeSats from the ISS. The first data gathered from the satellite was April 15, 2021. Prior to this date, the satellites' health monitoring and initial operations were done to confirm that the satellites are working well. Unfortunately, we were only able to confirm proper operation with one of the satellites, Tsuru, where most of the data would come from. This satellite carries the Perovskite solar cell with CuSCN hole transport material. Hence, we weren't able to gather data from the Spiro-OMeTAD HTM and HTM free carbon electrode Perovskite solar cells.

Figure 49 Birds-4 satellites deployment from the International Space Station. This Deployment Image was taken by Astronaut Soichi Noguchi from ISS [51]

Left to Right: RSP-1, Tsuru, Maya-2, GuaraniSat-1,OpuSat

After processing the downloaded data and removal of invalid data sets, such as those taken during the time that satellite is not pointed towards the sun or in eclipse, or those with erroneous values, the first set of J-V curve data from the two CuSCN PSC samples attached to

the satellite gathered on April 15 are shown in Figure 50. The tabulated parameters of each set is shown in Table 5. From this set of data, it was observed that the sun angle measurements are inconsistent with the short circuit current and maximum power of the cells. Set 5 has a 90-degree angle measurement while set 3 and 6 have lower angle measurement but their short circuit current and maximum output power are relatively the same. This is mainly because of the rotation of the satellite which causes variation in irradiance received by the satellite during each measurement. The inconsistency of the photodiode sun sensor could be due to shadows casted by other parts of the Y-panel on the photodiode sun sensor. Hence, other methods are needed to be applied to identify the correct sun angle and irradiance during the measurement

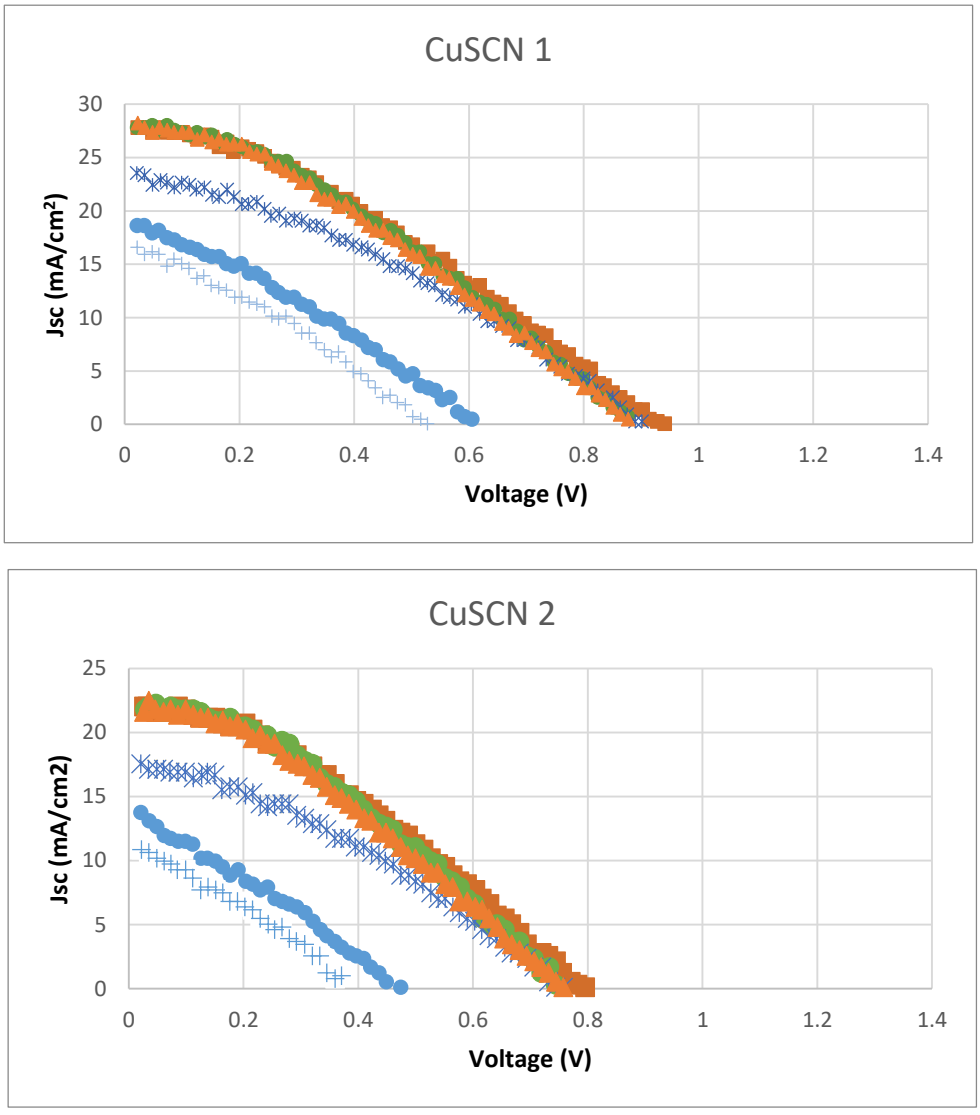

Figure 50 First set of J-V curve gathered from the satellite on April 15, 2021

of the perovskite solar cells.

Table 5 Measured parameters of the first set of data from the PSC mission

	CuSCN 1			CuSCN 2				
Set	Voc (V)	Jsc (mA/cm2)	Pmax (mW)	Voc (V)	Jsc (mA/cm2)	Pmax (mW)	Temp. (°C)	Angle (°)
1	0.95	27.81	8.59	0.81	22.03	5.92	10.98	25.46
2	0.62	18.64	3.55	0.46	13.75	1.91	8.24	78.63
3	0.89	28.03	8.03	0.76	22.25	5.51	14.77	13.89
4	0.54	16.61	2.85	0.38	10.83	1.32	12.92	86.24
5	0.91	23.56	7.14	0.77	17.56	4.53	16.38	90.00
6	0.89	28.25	8.21	0.77	22.47	5.54	17.43	3.88

It is known that there is a linear relationship between the amount of sunlight and the short circuit current of solar cells [49]. From this, we can use the short circuit current density as basis of the irradiance when the short circuit current density is measured. For this, the short circuit current density versus the irradiance of a CuSCN PSC is measured as shown in Figure 51. The trend line is then plotted using linear regression to derive the function which relates the short circuit current density and irradiance as shown in Figure 52. The highest measured short circuit current in-flight which is 30.5 mA, is then used to scale the ground data to match the solar cells in orbit. The derived function shown in Figure 53 is then used to compute the irradiance at the time of short circuit current.

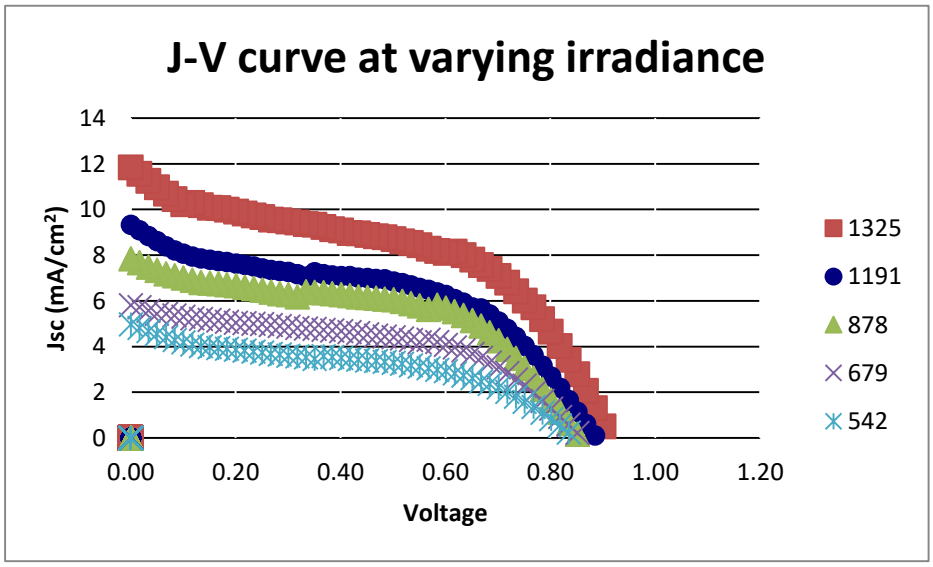

Figure 51 J-V curve at varying irradiance

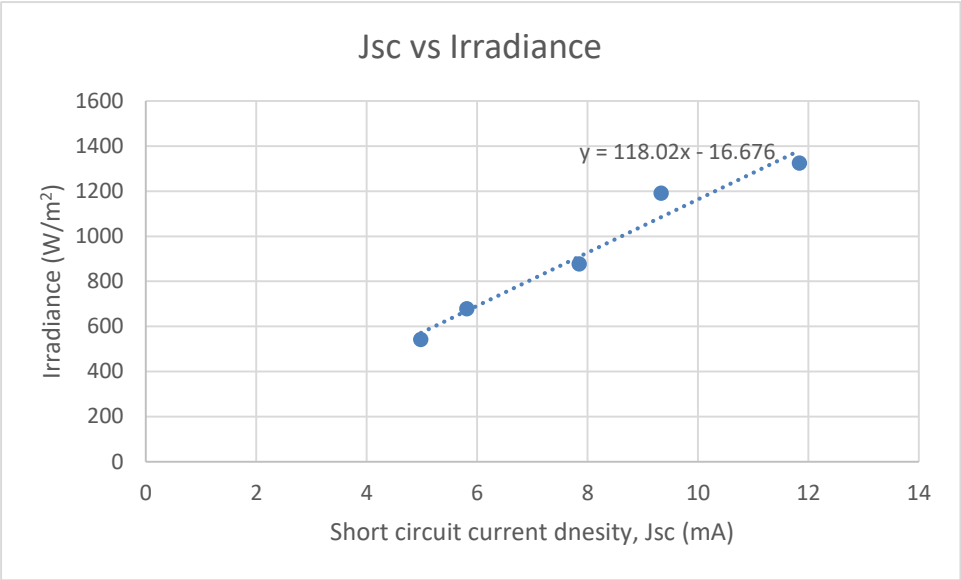

Figure 52 Plot of the linear relationship between Jsc and irradiance

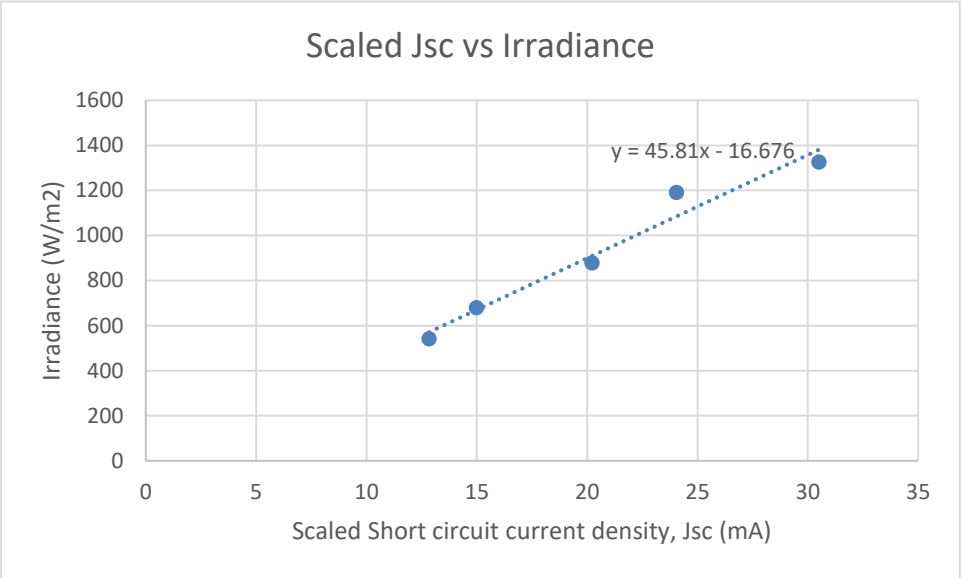

Figure 53 Jsc and irradiance relationship scaled with the gathered data from space

Since the satellite is rotating while the measurement is being done, the angle and irradiance when the Jsc is measured is different from the time the peak power was measured. From the measurements, it was identified that the average point when peak power is measured is at the 70th measurement out of 110 measurements. As mentioned at the beginning of chapter 5, the approximate time of each measurement is 12 seconds. That means that from the time the

short circuit current is measured (at the 110th measurement), approximately 5 seconds have passed since the peak power was measured. During the 5 months of operation of BIRDS-4 satellite, Tsuru, high sampling of housekeeping data was done sparingly. From this housekeeping data, we can derive the approximate rate of rotation during the execution of the perovskite solar cell mission and use that to adjust the sun angle and irradiance derived from the short circuit current density measurements. Shown in Figure 54 is a plot of the high sampling data and the derived rate of rotation across the Y-axis from where the Perovskite solar cell are attached. The decision on whether the adjustment is a plus- or a minus- to the sun angle depended on the value of maximum power. If the angle results to a high irradiance but the maximum power value is low, the angle is adjusted to reduce the irradiance derived and if the maximum power value is high, the angle is adjusted to increase the irradiance derived. This assures that the efficiency that will be calculated is reasonable.

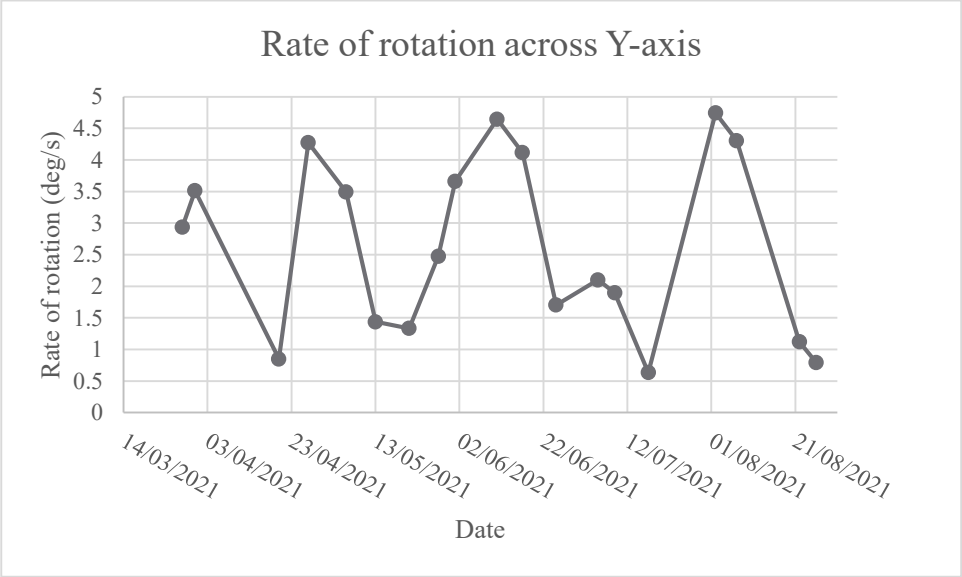

Figure 54 Average rate of rotation derived from the high sampling data obtained during various days it was executed

The maximum power measured from the CuSCN PSCs after 5 months of operation are shown in Figure 55. From the derived irradiance and the measured maximum power, the power conversion efficiency over time of the cells were calculated. Shown in Figure 56 is the PCE

over time of the CuSCN PSCs. To ensure that the values gathered are reasonable, the margin of error at a 95% confidence level of the measurements was calculated. The confidence interval is then juxtaposed with the measurement done, along with the trend line as shown in Figure 57. Most of the points lie in the confidence interval range, hence we can say these measurements are valid. Moreover, it can be observed that the trend line is decreasing over time, indicating a degradation of the samples in space. From this trend line, a slope of -0.023 and – 0.017 were derived, indicating an approximate reduction of 0.02% in PCE per day in-orbit. This degradation is significantly lower than the degradation observed during the ground tests. It

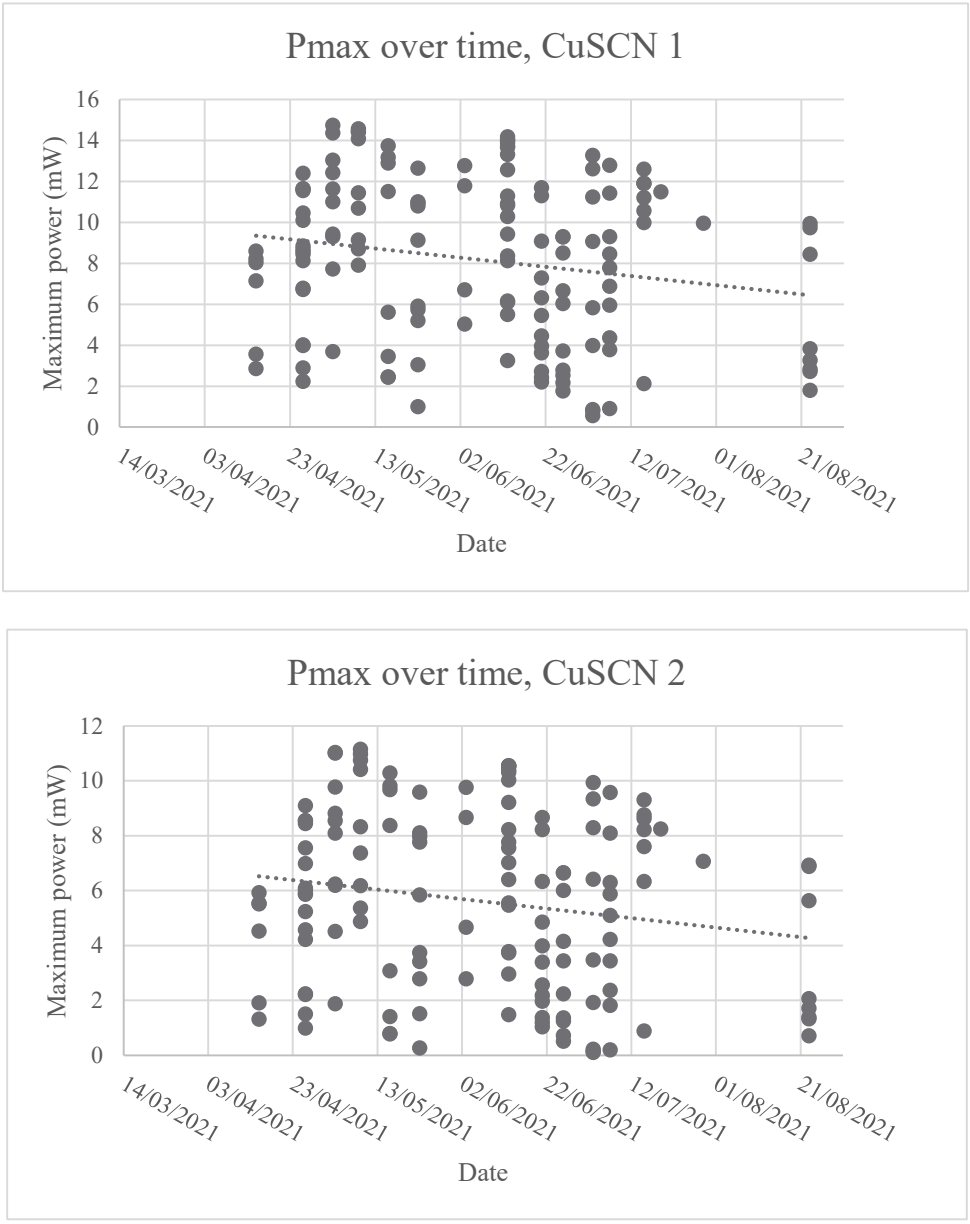

Figure 55 Plot of the measured maximum power from the CuSCN PSC

should be noted that the ground tests were done with fresh samples while the measurements in-orbit are aged samples. Degradation rate is higher with new samples since there are more elements to react with at the beginning than when the sample has aged already.

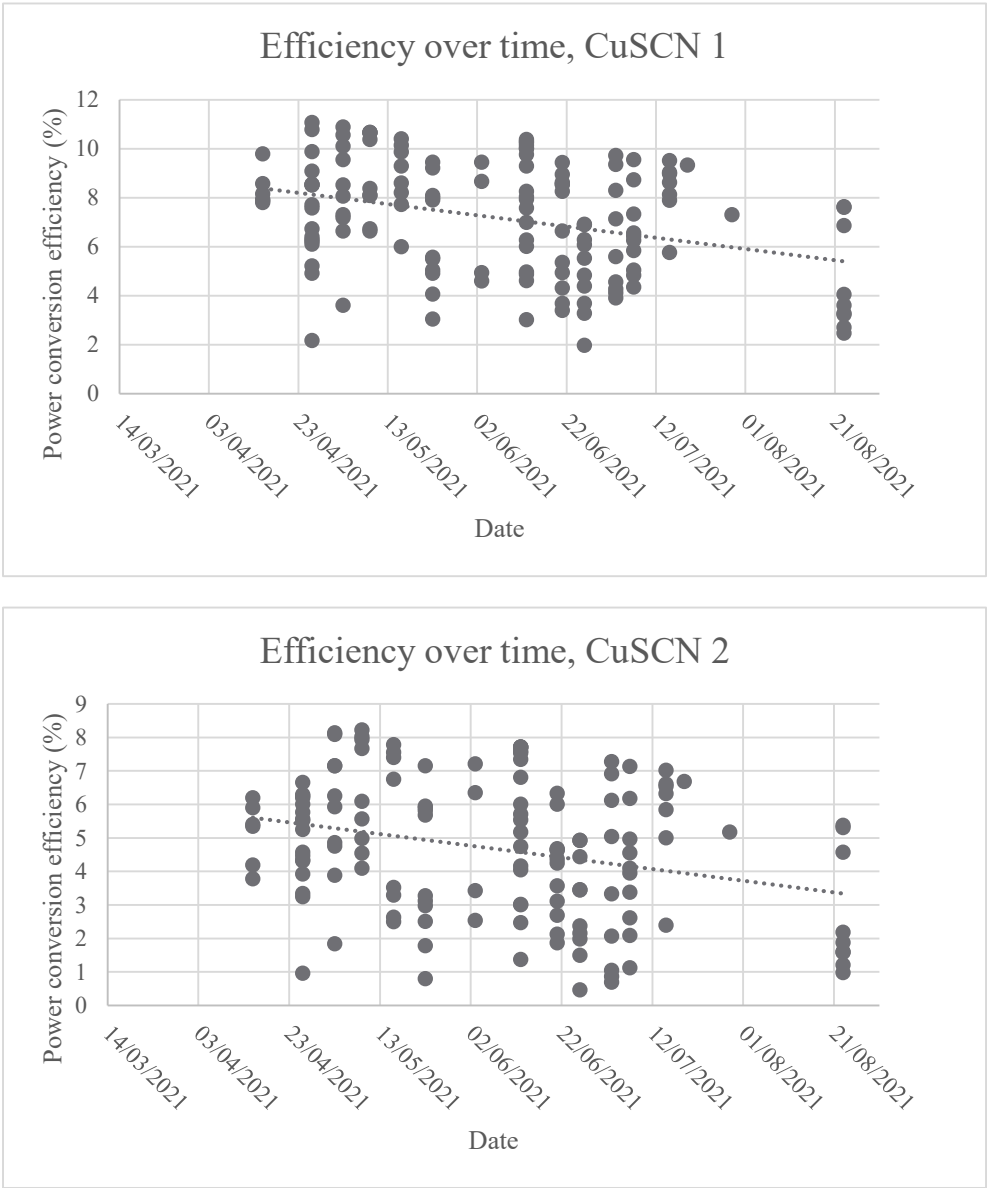

Figure 56 Efficiency over time of the CuSCN PSC

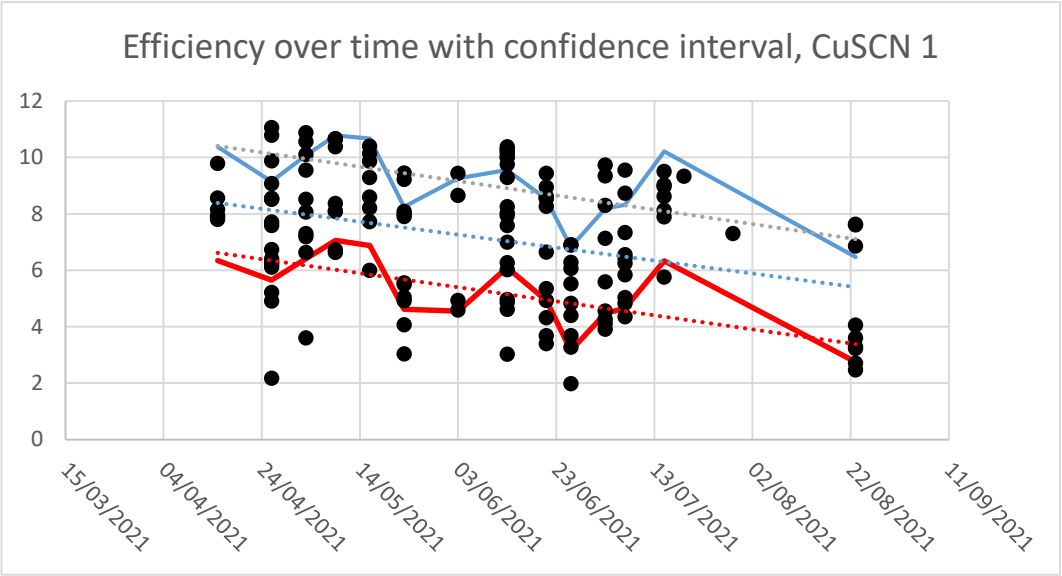

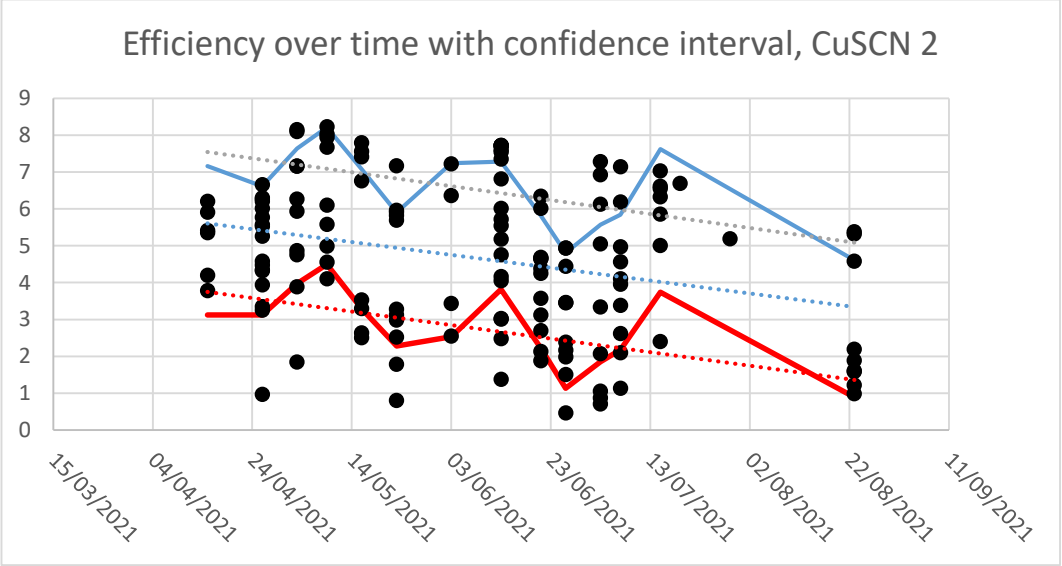

Figure 57 Margin of error plotted with the efficiency of the cells

From the average efficiency and the upper and lower bound values, the normalized efficiency with boundaries are plotted as shown in Figure 58. A degradation rate of -0.15% can be derived from the average efficiency of the CuSCN samples.

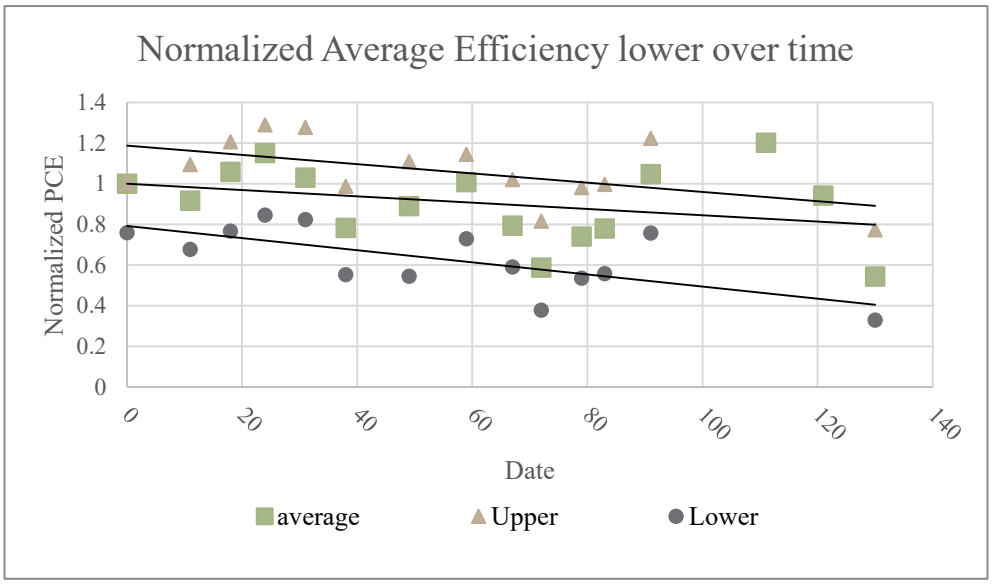

Figure 58 Normalized average, upper and lower bound efficiency of CuSCN space samples

Chapter 6: Comparison between Ground test and In-orbit data

Using least squares method, a linear equation is drawn from the average data points of the samples tested. Using these equations, the mean time to failure is calculated, where "failure" is defined as the time the power conversion efficiency goes below 70% of the initial value. Shown in Table 6 is a summary of the equations derived for each test and the calculated mean time to failure for each test, as well as in-orbit data results.

For the fresh samples, it can be observed by looking at the slope of the linear equation that the degradation rate per day is high compared to the aged CuSCN samples and the in-orbit data. The mean time to failure of the fresh samples are also short at about 8-15 days. For the aged CuSCN samples, it can be observed that the ground test results are not the same as the in-orbit data collected. For the thermal test with 35-minute cycle, the increased rate of thermal change introduces greater thermal shock and fatigue to the perovskite solar cell material compared to the 90 minute cycles. Even though the 90-minute thermal cycles produced significantly lower average normalized PCE degradation rate, it is still double that of what was observed in-orbit. One major factor is the presence of atmosphere during test that could contribute to the degradation of the material during thermal cycling. The researcher was supposed to test in a thermal vacuum chamber but unfortunately, all the devices broke down during the 90-minute thermal cycle test. This experiment is then left for future study. The vacuum test showed closer values to the in-orbit data. The difference could be pointed again to the presence of atmosphere when measurements are made. The lower and upper bound mean time to failure are at 30.6 days and 212 days, while the average mean time to failure of the space samples is computed at 199 days. From this derived MTTF, it can be inferred that CuSCN Perovskite solar cells can only function at more than 70% of their initial PCE for only 6 months, which is low for space solar cells standards.

Overall, the comparison of the ground test and in-orbit data showed difference in results. It is therefore advised for future study to do thermal vacuum that would mimic the same rate of thermal change in space. Characterization of the cells should be done inside the vacuum chamber to prevent the need of re-introducing humidity that could contribute to the degradation of cells and lead to inaccurate results. A small light source calibrated with a reference solar cell placed inside the thermal vacuum chamber would improve the overall accuracy of measurement and remove the need of repeated calibration of distance from the light source of the solar cells throughout the test proper which introduces uncertainties and errors during measurements. Applying these improvements could lead to closer values obtained between ground test and in-orbit data.

Table 6 Summary of equations and computed mean time to failure of ground test and in-orbit data

Test	Linear equation (X in days)	MTTF (days)
Fresh Spiro Thermal test 1	$-360E^{-4}X + 1.012$	8.33
Fresh CuSCN Thermal test 1	$-480E^{-4}X + 1.0$	6.25
Fresh Carbon Thermal test 1	$-375E^{-4}X + 0.934$	8.0
Fresh Spiro Vacuum test 2	$-360E^{-4}X + 1$	8.33
Fresh Carbon Vacuum test 2	$-192E^{-4}X + 1$	15.63
Aged CuSCN Thermal test 3 (-20 to 15°C) 35 min./cycle	$-105E^{-4}X + 1.017$	30
Aged CuSCN Thermal test 4 (-20 to 15°C) 90 min./cycle	$-30E^{-4}X + 0.999$	100

Aged CuSCN Vacuum test 3	$-22E^{-4}X + 0.989$	134
CuSCN samples Space data (upper bound)	$-23E^{-4}X + 1.188$	212
CuSCN samples Space data (lower bound)	$-30E^{-4}X + 0.792$	30.6
CuSCN samples Space data (average)	$-15E^{-4}X + 0.999$	199

Chapter 7: Conclusion

Perovskite solar cells have garnered significant attention in the past few years due to its high power density, low manufacturing cost and high power conversion efficiency which is near the current efficiency of triple junction solar cells that are being used in space applications. The thesis investigated the feasibility of Perovskite solar cells in space through ground tests simulating low-earth orbit space environment and in-orbit demonstration of PSCs through the BIRDS-4 satellite program. The results led to the following conclusions on each objective:

Objective 1. To obtain data on performance of PSC in Low Earth Orbit space environment in simulated space environment (ground test)

Prior to the launch of the satellites, ground test for simulated space conditions were done such temperature cycling, vacuum, UV radiation and vibration test to learn the performance of different PSCs made with Organic (Spiro-OMeTAD) HTM, inorganic (CuSCN) HTM and HTM free Carbon electrode PSC. Comparison on the performance of PSCs which used different HTM and back electrode show that even though PSCs with Spiro-OMeTAD have high initial PCE, their performance quickly degrades when exposed to the harsh space environment conditions. On the other hand, although HTM free PSC with carbon as back electrode showed lower initial PCE compared to PSCs which used organic and inorganic HTM, it showed superior lifespan and stability under the simulated space environment. The innate hydrophobic property and thermal stability, combined with the thicker layer it provides and low material cost showed it is a good candidate for future development of PSCs and towards its commercialization. The lower cost of using carbon compared to gold as back electrode and removal of the need for an HTM gives carbon more credit. This result corroborates with research reviewed in [50]. Further improvement on the encapsulation method is also seen to allow more stable PSCs with longer life span.

Objective 2. To prepare PSCs as BIRDS-4 satellites payload and design on-board system to measure and record the performance of PSCs in space (in-orbit)

To affirm the feasibility of PSCs under the harsh space environment, the BIRDS-4 project launched a constellation of three satellites in March of 2021, which carries PSCs to gather in-orbit data on the long term performance of PSCs in space. The satellites carried a different type of PSC with two (2) samples each. Unfortunately, the BIRDS-4 team was only able to gather data from the Japanese satellite, Tsuru, carrying PSC with CuSCN inorganic HTM. Data gathered from April 15, 2021 until August 23, 2021 was analysed in this paper which shows slower degradation rate of -0.15% per day from the normalized initial power conversion efficiency compared with the ground test done with fresh samples. It is inconclusive what caused the slowdown of degradation and one hypothesis is the ageing of the cells prior to launch in space allowed for stabilization of the cells which resulted to slower reaction and degradation with the environment.

Objective 3. To compare in-orbit data with ground data in terms of their predicted lifespan.

Using ground data and in-orbit data, linear and exponential equations were derived using least squares method which allowed estimation of the mean time to failure of the perovskite solar cells, where failure is described as 30% reduction of the original power conversion efficiency. From the results, it shows that ground tests done with aged cells did not have the same MTTF as those in space.

Overall, the research was able to establish ground work on the feasibility study of Perovskite solar cells in space and give direction on which areas should be further explored and improved towards the goal of realizing the use of Perovskite solar cells in space.

Recommendations for Future research

For future research, it is recommended to find other materials that would be more stable under atmospheric environment. A combination of CuSCN HTM and Carbon back electrode could show better results in terms of PCE, lifespan and stability. Improving the encapsulation method that would use more advanced machineries to seal and isolate the cell from the external environment is also recommended. This would ensure that the cells would maintain their initial PCE prior to launch to space.

Improvements in the ground test methodology such as using a fixed light source to solar cell setup is recommended to reduce inaccuracies during measurement. Having a test setup where measurement can be made continuously while the cells are inside a thermal vacuum chamber could result to closer results with in-orbit data. Increasing the number of test samples, both for ground test and in-orbit demonstration would also help gain statistically significant conclusions.

Further research on the actual cause of the slowdown in degradation of space samples could lead to increasing the lifespan and feasibility of usage PSCs in space. Future satellite missions that aims to gather in-orbit data on perovskite solar cells are recommended to have more frequency in measuring the sun intensity to reduce uncertainty in the calculation of PCE from the data gathered.

Lastly, larger perovskite solar cells or modules that could generate significant amount of energy can be attached to the satellite would also be a good direction of research to prove the practicality and capability of PSC to replace existing solar cells being used in satellite missions.

References

[1] NREL, "Best research-cell efficiencies multijunction cells," 26 july 2021. [Online]. Available: https://www.nrel.gov/pv/assets/pdfs/cell-pv-eff-mjcells-rev210726.pdf. [Accessed 9 september 2021].

[2] NREL, "Best research-cell efficiencies crystalline silicon," 26 july 2021. [Online]. Available: https://www.nrel.gov/pv/assets/pdfs/cell-pv-eff-crysi-rev210726.pdf. [Accessed 9 september 2021].

[3] C. Meehan, "SolarReviews," 18 july 2018. [Online]. Available: https://www.solarreviews.com/blog/nrel-developing-tech-lower-cost-multi-junction-solar-cells. [Accessed 9 September 2021].

[4] A. Kojima, K. Teshima, Y. Shirai and T. Miyasaka, "Organometal Halide Perovskites as Visible-Light Sensitizers for Photovoltaic Cells," *Journal of the American Chemical Society,* pp. 6050-6051, 2009.

[5] NREL, "Best research-Cell efficiency chart emerging PV," 26 July 2021. [Online]. Available: https://www.nrel.gov/pv/assets/pdfs/cell-pv-eff-emergingpv-rev210726.pdf. [Accessed 9 September 2021].

[6] F. M. and E. B., "Efficiency Limit of Perovskite/Si Tandem Solar cells," *ACS Energy Letters,* vol. 1, pp. 863-868, 31 January 2016.

[7] M. Kaltenbrunner, M. White, E. Głowacki, T. Sekitani, T. Someya, N. Sariciftci and S. Bauer, "Ultrathin and lightweight organic solar cells with high flexibility," *Nature communications,* vol. 3, no. 770, p. 7, 03 April 2012.

[8] N. Chang, A. Y. Ho-Baillie, D. Vak, M. Gao, M. Green and R. Egan, "Manufacturing cost and market potential analysis of demonstrated roll-to-roll perovskite photovoltaic cell processes," *Solar Energy Materials and Solar cells,* vol. 174, pp. 314-324, 2018.

[9] Y. Miyazawa, M. Ikegami, H. Chen, T. Ohshima, M. Imaizumi, K. Hirose and T. Miyasaka, "Tolerance of Perovskite Solar cell to high-energy particle irradiations in space environment," *iScience,* no. 2, pp. 148-155, 2018.

[10] Q. Wang, B. Chen, Y. Liu, Y. Deng, Y. Bai, Q. Donga and J. Huang, "Scaling behavior of moisture-induced grain degradation in polycrystalline hybrid perovskite thin films," *Energy and Environmental science,* no. 2, 2017.

[11] Z. Song, A. Abate, S. C. Watthage, G. K. Liyanage, A. B. Phillips, U. Steiner, M. Graetzel and M. J. Heben, "Perovskite Solar Cell Stability in Humid Air: Partially Reversible Phase Transitions in the PbI2-CH3NH3I-H2O System," *Advanced energy materials,* vol. 6, no. 19, 2016.

[12] J. Yang, Q. Bao, L. Shen and L. Ding, "Potential applications for perovskite solar cells in space," *Nano Energy,* vol. 76, no. June, 2020.

[13] A. D. Sheikh, R. Munir, M. A. Haque, A. Bera, W. Hu, P. Shaikh, A. Amassian and T. Wu, "Effects of High Temperature and Thermal Cycling on the Performance of Perovskite Solar Cells: Acceleration of Charge Recombination and Deterioration of Charge Extraction," *ACS Applied Materials and Interfaces,* vol. 9, no. 40, pp. 35018-35029, 2017.

[14] S.-W. Lee, S. Kim, S. Bae, K. Cho, T. Chung, L. E. Mundt, S. Lee, S. Park, H. Park, M. C. Schubert, S. W. Glunz, Y. Ko, Y. Jun, Y. Kang, H.-S. Lee and D. Kim, "UV Degradation and Recovery of Perovskite Solar Cells," *Scientific reports,* vol. 6, 2016.

[15] S. Pitchaiya, M. Natarajan, A. Santhanam, V. Asokan, A. Yuvapragasam, V. M. Ramakrishnan, S. E. Palanisamy, S. Sundaram and D. Velauthapillai, "A review on the classification of organic/inorganic/carbonaceous hole transporting materials for perovskite solar cell application," *Arabian Journal of Chemistry,* no. 13, pp. 2526-2557, 2018.

[16] "Sigma-Aldrich," [Online]. Available: https://www.sigmaaldrich.com/united-states.html. [Accessed 30 September 2020].

[17] H.-R. Wenk and A. Bulakh, Minerals: Their Constitution and Origin, New York: Cambridge University Press, 2004.

[18] "Perovskite mineral data," [Online]. Available: http://webmineral.com/data/Perovskite.shtml#.YTk_7Y4zZPa. [Accessed 9 september 2021].

[19] M. M. Lee, J. Teuscher, T. Miyasaka, T. Murakami and H. Snaith, "Efficient Hybrid solar cells based on Meso-superstructured organometal halide perovskites," *Science,* no. 338, pp. 643-647, 2012.

[20] I. Hussain, H. Tran and J. e. a. Jaksik, "Functional materials, device architecture and flexibility of perovskite solar cell," *emergent material,* no. 1, pp. 133-154, 2018.

[21] N. Marinova, S. Valero and J. Delgado, "Organic and perovskite solar cells: Working principles. materials and interfaces," *Journal of Colloid and Interface Science,* vol. 488, pp. 373-389, 2017.

[22] L. Huang, Z. Hu, JieXu, K. Zhang, J. Zhang, J. Zhang and Y. Zhu, "Efficient and stable planar perovskite solar cells with a non-hygroscopic small molecule oxidant doped hole transport layer," *Electrochimica Acta,* vol. 196, pp. 328-336, 2016.

[23] Z. Hawash, L. K. Ono and Y. Qi, "Recent Advances in Spiro-MeOTAD Hole Transport Material and Its Applications in Organic–Inorganic Halide Perovskite Solar Cells," *Advanced Materials Interfaces,* vol. 5, no. 1, 2017.

[24] U. Bach, D. Lupo, P. Comte, J. Moser, F. Weissortel, J. Salbeck, H. Spreitzer and M. Gratzel, "Solid-state dye-sensitized mesoporous TiO 2 solar cells with high photon-to-electron conversion efficiencies," *Nature,* no. 395, pp. 583-585, 1998.

[25] J. Christians, R. Fung and P. Kamat, "An inorganic hole conductor for organo-lead halide perovskite solar cells Improved hole conductivity with copper iodide.," *J. Am. Chem. Soc.,* vol. 136, pp. 758-764, 2014.

[26] S. Chavhan, O. Miguel, H.-J. Grande, V. Gonzalez-Pedro, R. Sanchez, E. Barea, I. Mora-Sero and R. Tena-Zaera, "Organo-metal halide perovskite-based solar cells with CuSCN as the inorganic hole selective contact," *J. Mater. Chem. A,* vol. 2, pp. 12754-12760, 2014.

[27] S. Ito, S. Tanaka, H. Vahlman, H. Nishino, K. Manabe and P. Lund, "Carbon-Double-Bond-Free Printed Solar Cells from TiO2/CH3NH3PbI3/CuSCN/Au: Structural Control and Photoaging Effects," *ChemPhysChem,* vol. 15, no. 6, pp. 1194-1200, 2014.

[28] R. Zhao, B. Yan, Y. Yang, T. Kim and A. Amassian, "Solution-processed inorganic copper(I) thiocyanate (CuSCN) hole transporting layers for efficient p-i-n perovskite solar cells," *J. Mater. Chem. A,* vol. 3, pp. 20554-20559, 2015.

[29] Y. Yang, J. Xiao, H. Wei, L. Zhu, D. Li, Y. Luo, H. Wu and Q. Meng, "An all-carbon counter electrode for highly efficient holeconductor-free organo-metal perovskite solar cells.," *RSC Adv.,* vol. 4, pp. 52825-52830, 2014.

[30] F. Zhang, X. Yang, M. Cheng, W. Wang and L. Sun, "Boosting the efficiency and the stability of low cost perovskite solar cells by using CuPc nanorods as hole transport material and carbon as counter electrode," *Nano Energy,* no. 20, pp. 108-116, 2016.

[31] J. A. Schwenzer, L. Rakocevic, R. Gehlhaar, T. Abzieher, S. Gharibzadeh, S. Moghadamzadeh, A. Quintilla, B. S. Richards, U. Lemmer and U. W. Paetzold, "Temperature variation-induced performance decline of perovskite solar cells," *ACS materials and Interfaces,* vol. 10, pp. 16390-16399, 2018.

[32] X. Zhao and N. Park, "Stability issues on perovskite solar cells," *Photonics,* vol. 2, no. 4, pp. 1139-1151, 2015.

[33] L. T., E. G.E., P. S., A. Abate, M. Lee and H. Snaith, "Overcoming ultraviolet light instability of sensitized TiO2 with meso-superstructured organometal tri-halide perovskite solar cells," *Nature Communication,* 2013.

[34] Y. J. Hofstetter, I. García-Benito, F. Paulus, S. Orlandi, G. Grancini and Y. Vaynzof, "Vacuum-induced degradation of 2D Perovskites," *Frontiers in Chemistry,* vol. 8, pp. 1-10, 2020.

[35] Y. Jiang, S. C. Yang, Q. Jeangros, S. Pisoni, T. Moser, S. Buecheler, A. N. Tiwari and F. Fu, "Mitigation of vacuum and illumination-induced degradation in Perovskite solar cells by structure engineering," *Joule,* vol. 4, no. 5, pp. 1087-1103, 2020.

[36] R. Funase, E. Takei, Y. Nakamura, M. Nagai, A. Enokuchi, C. Yuliang, K. Nakada, Y. Nojiri, F. Sasaki, T. Funane, T. Eishima and S. Nakasuka, "Technology demonstration on University of Tokyo's picosatellite "XI-V" and its effective operation result using ground station network," *Acta Astronautica,* vol. 61, pp. 707-711, 2007.

[37] C. Morioka, K. Shimazaki, S. Kawakita, M. Imaizumi, H. Yamaguchi, T. Takamoto, S. Sato, T. Ohshima, Y. Nakamura, K. Hirako and M. Takahashi, "First flight demonstration of film-laminated InGaP/GaAs and CIGS thin film solar cells by JAXA's small satellite in LEO," *Progress in Photovoltaics: Research and applications,* vol. 19, pp. 825-833, 2011.

[38] K. Okada, Y. Seri, R. Shibagaki, H. Masui and M. Cho, "Ground Tests and In-Orbit Results for the Horyu-II Nanosatellite Power System," *Transactions of the Japan Society for Aeronautical and Space Sciences, Aerospace Technology Japan,* vol. 12, pp. 49-56, 2014.

[39] I. Cardinaletti, T. Vangerven, S. Nagels, R. Cornelissen, D. Schreurs, J. Hruby, J. Vodnik, D. Devisscher, J. Kesters, J. D'Haen, A. Franquet, V. Spampinato, T. Conard, W. Maes, W. Deferme and J. V. Manca, "Organic and perovskite solar cells for space applications," *Solar energy materials and solar cells,* vol. 182, pp. 121-127, 2018.

[40] L. K. Reb, A. Meyer, L. K. Reb, M. Bo, B. Predeschly, S. Grott, C. L. Weindl, G. I. Ivandekic, R. Guo, C. Dreißigacker, R. Gernha and A. Meyer, "Report Perovskite and Organic Solar Cells on a Rocket Flight Perovskite and Organic Solar Cells," *Joule,* vol. 4, pp. 1-13, 2020.

[41] K. Herrick, "Building Solar Panels in space might be as easy as clicking print," 31 October 2019. [Online]. Available: https://www.nasa.gov/feature/glenn/2019/buildingsolar-panels-in-space-might-be-as-easy-as-clicking-print. [Accessed 1 July 2021].

[42] F. Matteocci, L. Cinà, E. Lamanna, S. Cacovich, G. Divitini, P. A. Midgley, C. Ducati and A. D. Carlo, "Encapsulation for long-term stability enhancement of perovskite solar cells Fabio," *Nano Energy,* vol. 30, pp. 162-172, 2016.

[43] M. Galarynk, "towards data science," 12 September 2018. [Online]. Available: https://towardsdatascience.com/understanding-boxplots-5e2df7bcbd51. [Accessed 30 June 2021].

[44] J. Christians, J. Manser and P. Kamat, "Best Practices in Perovskite solar cell efficiency measurements: Avoiding the error of making bad cells look good," *J. Phys. Chem. Lett.,* vol. 6, pp. 852-857, 2015.

[45] Tindo solar, "tindosolar.com.au," [Online]. Available: https://www.tindosolar.com.au/learn-more/temperature-coefficient/#:~:text=As%20a%20solar%20panel%20increases,every%20degree%20the%20temperature%20rises.. [Accessed 7 September 2020].

[46] A. Aho, R. Isoaho, A. Tukiainen, V. Polojarvi, T. Aho, M. Raappana and M. Guina, "Temperature coefficients for GaInP/GaAs/GaInNAsSb solar cells," in *AIP Conference Proceedings*, 2015.

[47] R. Cheacharoen, N. Rolston, D. Harwood, K. Bush, R. H. Dauskardt and M. D. McGehee, " Design and understanding of encapsulated perovskite solar cells to withstand temperature cycling," *Energy Environ. Sci.,* vol. 11, p. 144, 2018.

[48] C. Ramirez, S. Yadavalli, H. Garces, Y. Zhou and N. Padture, "Thermo-mechanical behavior of organic-inorganic halide perovskite for solar cells," *Script Materialia,* vol. 150, pp. 36-41, 2018.

[49] M. Batzill and U. Diebold, "The surface and materials science of tin oxide," *Prog. Surf. Sci.,* vol. 79, pp. 47-154, 2005.

[50] W. Wu and B. Chiou, "Mechanical properties of r.f. magnetron sputtered indium tin oxide films," *Thin Solid Films,* vol. 293, pp. 244-250, 1997.

[51] D. Han, S. Yi, Q. Yuan, X. Tang, Q. Shu, Q. Li, F. Wang and D. Zhou, "Managing defects density and interfacial strain via udnerlayer engineering for inverted CsPbI2Br Perovskite solar cells with all-layer dopant-free," *Small,* vol. 17, no. 28, 2021.

[52] Y. Shen, F. Wang and Q. Wang, "Ultralow thermal conductivity and negative thermal expansion of CuSCN," *Nano Energy,* vol. 73, 2020.

[53] Engineering Toolbox, "Thermal Expansion - Linear Expansion Coefficients [online]," 2003. [Online]. Available: https://engineeringtoolbox.com/linear-expansion-coefficients-d_95.html. [Accessed 9 November 2021].

[54] F. A. Roghabadi, N. M. R. Fumani, M. Alidaei, V. Ahmadi and S. M. sadrameli, "High power UV-Light Irradiation as a New Method for Defect passivation in Degraded perovskite solar Cells to Recover and enhance the performance," *Scientific reports,* vol. 9, 2019.

[55] M. Liu, M. Endo, A. Shimazaki, A. Wakamiya and Y. Tachibana, "Light Intensity Dependence of Performance of Lead Halide Perovskite Solar Cells," *Journal of Photopolymer Science and Technology,* vol. 30, no. 5, pp. 577-582, 2017.

[56] M. Hadadian, J.-H. Smått and J.-P. and Correa-Baena, ": The role of carbon-based materials in enhancing the stability of perovskite solar cells," *Energy envrion. Sci,* vol. 13, pp. 1377-1407, 2020.

[57] S. [. Noguchi, "Small Satellites were successfully deployed [Tweet]," 14 March 2021. [Online]. Available: https://twitter.com/Astro_Soichi/status/1371070358015537155/photo/1. [Accessed 6 June 2021].